INTERNATIONAL JOURNAL FOR NUMERICAL AND ANALYTICAL METHODS IN GEOMECHANICS, VOL. 21, 753–787 (1997)

THE ROLE OF NON-LINEAR DEFORMATION ANALYSES IN THE DESIGN OF A REINFORCED SOIL BERM AT RED RIVER U-FRAME LOCK NO. 1

ROBERT M. EBELING, JOHN F. PETERS*, AND REED L. MOSHER

U.S. Army Engineer Waterways Experiment Station, 3909 Halls Ferry Road, Vicksburg, MS 39180-6199, U.S.A.

SUMMARY

This paper describes a design application of non-linear deformation analysis to a complex soil–structure–foundation interaction problem through use of a finite element analysis. The problem consists of a proposed renovation to an existing soil-founded U-frame lock structure consisting of construction of a densely reinforced soil berm adjacent to an existing lock wall. Major questions facing the designer involve reduction of the earth pressure on the lock wall, layout of the reinforcing in the soil berm, and collateral effects of berm construction on the U-frame lock structure. A non-linear deformation analysis played a central role in addressing all of these questions. Berm construction and four operational load cases were used to understand the performance of the reinforced berm and to discern interactions among the lock, the backfill, the foundation strata of the U-frame lock, the reinforced berm, and the foundation strata of the reinforced berm. Insight gained from the soil–structure–foundation interaction analyses led to an alteration to the proposed reinforcement layout to enhance the performance of the reinforced soil berm.

Int. J. Numer. Anal. Meth. Geomech., Vol. 21, 753–787 (1997)
(No. of Figures: 22 No. of Tables: 1 No. of Refs: 24)

Key words: finite element; soil structure interaction; soil reinforcement

1. INTRODUCTION

The importance of deformations in the analysis of earth pressures was recognized early in this century by Terzaghi.[1] However, until the general availability of the finite element method, the role of deformations was assessed qualitatively in the interpretation of empirical pressure diagrams (e.g. for braced excavations). Deformations also play an important role in limit equilibrium analyses because a factor of safety is computed for a predefined failure mechanism. In a complex retaining structure, the critical mechanism(s) may be difficult to anticipate without a deformation analysis, particularly if flexural structural members (e.g. the base slab and the stem walls of a U-frame lock) are present. Finally, in some problems the deformation is of principal interest. Therefore, unless there is strong precedent for a particular retaining structure or unless there is latitude for application of the observational construction technique, design of complex retaining structures should include deformation analysis.

*Correspondence to J. F. Peters, U.S. Army Engineer Waterways Experiment Station, 3909 Halls Ferry Road, Vicksburg, MS 39180-6199, U.S.A.

CCC 363–9061/97/110753–35$17.50

Received 5 September 1995
Revised 20 February 1997

This paper presents a soil–structure interaction study conducted to assess potential lock performance with the reinforced soil berm adjacent to the riverside lock wall.[2] The soil–structure–foundation interaction study was conducted in two phases: development of a finite element model and comparison of results with instrumentation measurements (a calibration study) and evaluation of the performance of the proposed reinforced berm with regard to its interaction with the lock, backfill, and the surrounding foundation soil strata (an assessment of the reinforced berm). The reinforced berm study discussed in this paper demonstrated how simulated Soil–Structure Interaction (SSI) modelling can be used to: (1) understand the performance of the reinforced berm and the sometimes complex interactions among the lock, the backfill, the foundation strata of the U-frame lock, the reinforcement and the reinforced soil berm, and the foundation strata of the reinforced berm for five load cases, and (2) alter the design of the reinforcement layout to enhance overall performance of the lock/berm structure. It is also noted that even though measured performance data were used to calibrate the FEM model, new loading could extend the soil into the virgin compression regime thus limiting the applicability of the calibration data.

Lock and Dam No. 1 on the Red River Waterway in Louisiana has experienced a serious sediment problem since its completion in 1983. During high-water periods, sediments are being deposited against the riverside lock wall at a much faster rate and to a level greater than that anticipated during the design of the project. During a period of high water in the Spring of 1985, silt deposition against the riverside lock wall was as much as 14 ft (4·27 m) higher than that assumed in the design of the lock. While the deposition of silt caused no damage to the lock, it was felt that the silt should be removed before the river receded. Since the highest level of water in the river resulted from a less than 10 yr flood, the silt deposition will continue to be a problem, resulting in expensive maintenance costs in the future.

Placement of rock dikes and other hydraulic changes have somewhat alleviated the siltation problem in the lock approaches. A recent study considered concepts for a permanent solution. Construction of a reinforced soil berm next to the riverside lock wall showed the best potential for a permanent, low-maintenance solution. The goal for this design is to provide 'pressure relief' from the silt. Essentially, the berm would carry the weight (and lateral thrust) of the silt and be structurally independent from the stem portion (identified in Figure 1) of the lock wall, which is

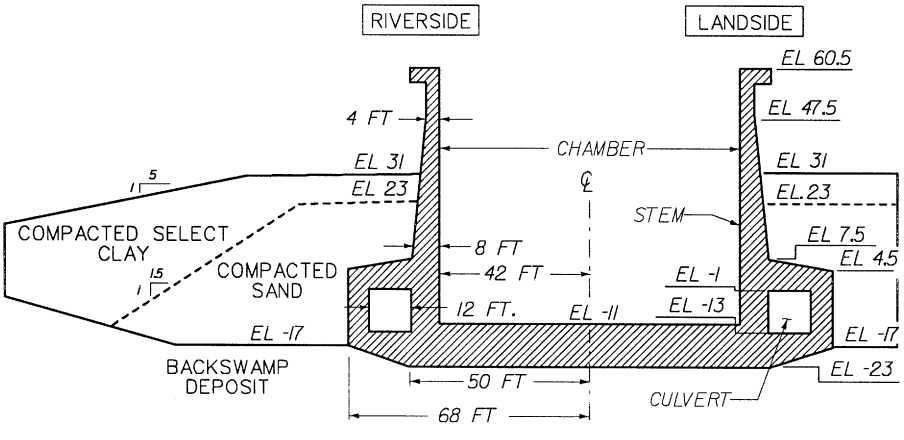

Figure 1. Cross section through monolith L-10 (1 ft = 0·305 m)

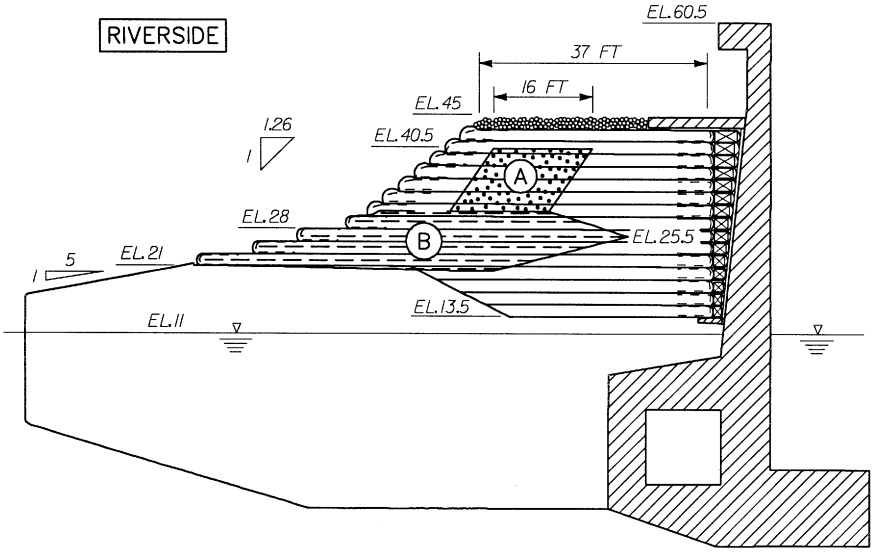

Figure 2. Riverside reinforced berm with lower pool and pool in lock at el 11 ft (1 ft = 0·305 m)

shown in Figure 2 with the proposed riverside berm. Structural independence would be achieved in this design by including a gap between the berm and the wall. The material shown filling the gap in Figure 2 has negligible stiffness and was not included in this analysis. Hence, the gap is shown as open in subsequent figures.

2. SITE LOCATION AND CONDITIONS

2.1. Location

The Red River Lock and Dam No. 1 is the first of a series of locks and dams to provide navigation between the Mississippi River and Shreveport, LA. Red River Lock and Dam No. 1 is located in central Louisiana, approximately 9 mile (14·4 km) upstream from the confluence of the Red and Black Rivers.

2.2. Conditions

Lock No. 1 is a reinforced concrete U-frame structure founded directly on the foundation soil strata with no bearing piles. The navigation chamber is 84 ft (25·6 m) wide by 685 ft (208.78 m) long. Figure 1 shows a cross section through the existing lock monolith No. L-10, located midway along the lock chamber. The structure was constructed with compacted sand select compacted clay backfill on each side of the culvert and stem walls to an elevation of 31 ft (9·45 m).

The site comprises the Point Bar Deposit, the Backswamp Deposit, and the sand substratum. The three strata are idealized in Figure 3 (details regarding variations within strata are not shown) for the corresponding finite element mesh used in the soil–structure interaction analyses. The deepest deposit is the sand substratum and comprises mainly dense sands with some gravel.

The Point Bar Deposit is predominantly silt, with regions of silty sand and poorly graded sand deposits. The Backswamp deposit consists predominantly of overconsolidated CH clays (by the Unified Soil Classification System), but also contains interbedded layers of lean clays (CL), silts, silty sands, and sands.

3. INITIAL DESIGN OF THE REINFORCED SOIL BERM

The initial reinforcement layout was designed using limit equilibrium procedures. The principal concerns in the design were (1) to provide an adequate factor of safety against the deep-seated failure of the foundation–berm system, (2) to provide stability to the steep berm faces, and (3) to limit the transfer of earth pressure to the lock wall. The third item is the focus of the deformation analysis described in following sections. Figure 3 shows the critical deep-seated failure surface for the reinforced soil berm used in the design. The reinforcement depicted in Figure 3 provides the minimum allowable factor of safety against slope failure for the berm of 1·25 for short-term loading and 1·5 for long-term loading. The reinforcement layout varies throughout the berm and consists of a total of 28 primary and secondary layers. Each primary layer extends across the entire width of the berm and is spaced every 1·5 ft (0·46 m) in elevation. The two zones of secondary reinforcement, labeled A and B in Figure 2, provide additional reinforcement along the face of the riverside slope. These secondary reinforcement layers were spaced at every 2 ft (0·61 m) in elevation (approximately) in region A and at every 1·5 ft (0·46 m) in elevation in region B.

4. SOIL–STRUCTURE INTERACTION ANALYSES

Engineering application of soil–structure interaction modelling requires a balance between modelling realism and simplicity. There is now over 25 yr experience in modelling construction procedures by the finite element method and the key ingredients in engineering application are

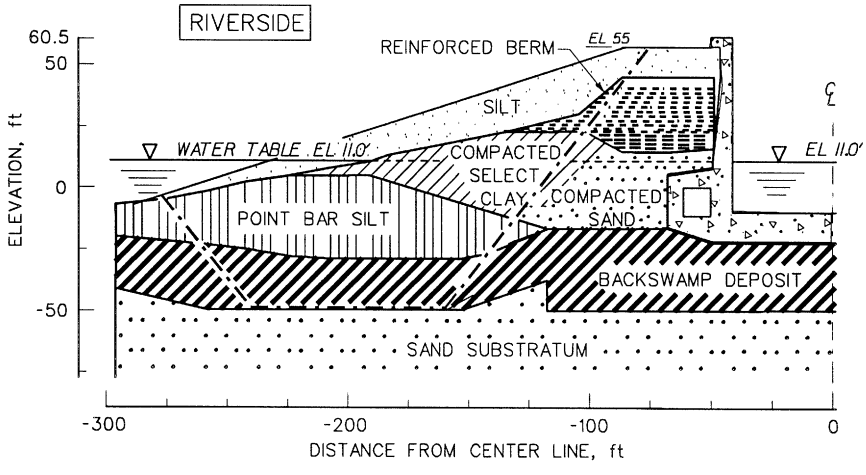

Figure 3. Critical slip surface within the reinforced berm with silt loading (1 ft = 0·305 m)

well known. This section describes the issues of modelling and material property determination that were important in the present analysis.

4.1. Analysis description

SOILSTRUCT[3] is a special-purpose, finite element program for two-dimensional, plane strain analysis of soil–structure interaction and soil-inclusion interaction problems. It calculates displacements and stresses resulting from incremental construction, excavation, dewatering, and/or load application. Non-linear, stress-path-dependent, stress–strain behaviour of the backfill and foundation soils was approximated in the finite element analyses using the tangent modulus method. In the tangent modulus method, new values of tangent moduli are assigned to each soil element at each increment of loading (i.e. dewatering, lock construction and backfilling) or unloading (i.e. excavation).

The key to a complex soil–structure interaction problem for engineering design is understanding which details must be modelled accurately and which do not. It is clearly critical that site geology is accurately interpreted from a geotechnical viewpoint and it has been found by experience that construction sequence is a determining factor in accurate non-linear analyses. In view of the intense research on constitutive equations of soils, the applicability of the simplistic hyperbolic model is worth reviewing.

The hyperbolic model of the SOILSTRUCT program has many deficiencies. The hyperbolic model is a pseudo-elastic non-linear model that captures inelasticity by distinguishing between loading and unloading stiffness modulii. As for isotropically hardening plasticity models, loading and unloading is determined by comparison of the stress state to an isotropic yield surface. In contrast to plasticity, the principal axes of the strain increment and stress increment coincide. Also, the incremental stiffness matrix is merely that of an isotropic elastic material but with the two stiffness moduli modified as loading proceeds to capture non-linearity. Therefore, coupling effects that give rise to shear-induced contraction and dilatancy are not captured. Finally, some implementations of the model use past maximum shear stress to detect load–unload–reload conditions which may not model behaviour of frictional materials in certain loading cases such as surcharging followed by surcharge removal, followed by loss of lateral constraint.

Despite these deficiencies, the hyperbolic model still finds application in engineering analysis. Undoubtedly, the model has popularity because its calibration is straight forward and its use has a large experience base. For the problems described in this report, the model finds applicability because it captures key elements of design. The model is typically used in the context of a total stress analysis for undrained materials or effective stress analysis for fully drained materials. Thus, the inability to model volume change properly is not a major issue. For soil–structure interaction problems, soil failure is typically limited to active stress conditions behind flexible walls where the failure state is reached with limited strain. Thus, errors in modelling kinematics are not a major concern. What are critical, and what the hyperbolic model captures well, are initial modulus, the loss of stiffness as stress levels approach yields conditions, and the stiffness variations of load–unload–reload cycles corresponding to cycles of active–passive earth pressure conditions during construction.

SOILSTRUCT has been used successfully in the past decade on several projects supported by field observations that illustrate these key points. One of the earliest successful applications of soil–structure interaction analysis was performed by Clough and Duncan[4,5] in their analysis of the two reinforced concrete U-frame locks at Port Allen and Old River. These two locks had been

extensively instrumented. Prior to Clough and Duncan's analyses, the instrumentation data had been thought to be unreliable and contrary to the perceived understanding of the behaviour of locks to loadings encountered during lock operation. Clough and Duncan's study showed that the best agreement between results computed using the finite element method and those obtained through instrumentation measurements is obtained when the actual construction process is simulated as closely as possible in the analysis. During their study, Clough and Duncan developed what is referred to as a *backfill placement analysis* in which the loads exerted by the backfill on the lock wall are generated automatically during simulated placement of backfill behind the wall.

Mosher and Knowles[6] modelled a tie-back diaphragm wall constructed through old slide debris. A goal of the analysis was to determine if excessive movements could occur behind the wall. Displacements were relatively small and good agreement was obtained between finite the element model and field instrumentation. The key difficulty was determining the properties of the slide debris. Parameters chosen for initial computations were shown by comparison to field instrumentation to be conservative although the computed displacements correctly predicted that movements would be well within specified limits. Mosher and Knowles also found that a major difficulty was to establish a statically consistent initial (pre-construction) stress state for the model. Because the site was both geologically and topographically complicated, initial stresses had to be established by a 'geneses' analyses whereby the formation of the site geology was modelled as a filling process.

Leavell et al.[7] analysed sheet pile walls to be used to increase effective levee height for flood control. Relatively large movements in soft foundation clays were expected and considerable effort was made to calibrate the finite element model against field loading tests. The hyperbolic model was calibrated using an empirical relationship between initial undrained stiffness and undrained shear strength. Despite several details that had to be considered in the model, the critical information needed to achieve agreement between model and field test was knowing the location of key soft-clay units within the foundation.

Mosher[8] applied the hyperbolic model to a three-dimensional version of SOILSTRUCT to model filling and flood loading of circular sheet pile cells. Modelling construction sequence and structural details were critical. Although the three-dimensional hyperbolic model required modification to a shear-bulk modulus description based on cubical triaxial tests, a suitable model was created that maintained the inherent simplicity of the original Duncan–Chang[9] model. Computed results were compared to empirical formulas for sheetpile cell design and instrumentation data for construction of Lock and Dam 26 on the Mississippi river. The finite element model gave good estimates for measured displacements and interlock forces. The results of Mosher have been used to improve empirical design methods for sheetpile cell structures.

4.2. Embedded elements

SOILSTRUCT has two types of reinforcement elements: standard bar elements intended for use as anchors, struts, and similar one-dimensional structural elements; and 'embedded' elements designed to model closely spaced reinforcement layers. The embedded element in the SOILSTRUCT version of Ebeling *et al.*[3] was developed as part of this project and used to model the 28 layers of reinforcement within the soil berm, as shown in Figure 5. Embedded element(s) are discrete bar element(s) embedded inside a soil berm element by coupling the bar's degree of freedom to those of the solid element through a compatibility relationship. Thus, the embedded

elements do not add to the total degrees of freedom. Details regarding the mathematical formulation of embedded elements, their use in soil-geoinclusion interaction problems, and experience gained when using this type of element to model instrumented retaining structures is discussed in detail in Appendix I.

There are two advantages of using the embedded element instead of the standard bar. First, because the layout of the embedded reinforcement is independent of the mesh design, a more regular mesh can be used. This feature significantly reduces the number of two-dimensional elements required for the model of the densely layered reinforced soil berm and its foundation regime. Prior to the development of embedded elements, SOILSTRUCT users were constrained in elevation to placement of solid soil element boundaries (i.e. nodes) at each layer of reinforcement (which were modelled using conventional bar elements). Some two-dimensional soil elements comprising the berm shown in Figure 5 contain up to six layers of reinforcement. The second advantage is that the assignment of reinforcement bars *within* each soil element can be automated by a straightforward search algorithm during the preprocessing phase of the finite element code, and the user needs only to supply data on the geometry of the reinforcement layers rather than data on the geometry of individual bar segments.

An obvious drawback to the embedded element is the assumption that slip does not occur between the element and soil. As discussed in detail is Appendix I, slip is not serious in densely spaced grids for which the method is intended. A computation of interface shear, which can be computed for the embedded element, showed that interface shear was insufficient to cause slip throughout the reinforced berm.

4.3. Material properties

4.3.1. Soil properties. SOILSTRUCT uses a hyperbolic representation for non-linear stress–strain relationship for soil, as described by Duncan and Chang.[9] Due to time and costs associated with sampling at a submerged site, additional field exploration and laboratory testing were not possible for this study. The authors were faced with the challenge of having to determine the hyperbolic constitutive model parameters from the limited data derived from the original laboratory testing programs performed during design and construction of the lock. Much of the data from the original testing program could not be used directly to determine the hyperbolic model parameters. Over the years, a large number of triaxial soil tests for different soils have been performed in which hyperbolic stress–strain model parameters have been extracted (see Reference 10). Because of the availability of these data and the authors's experience in applying the hyperbolic model to various types of soil, correlations were made with the test data from the original testing program to the data in the literature in order to assign the model parameters for the analysis. For example, the results of the standard penetration tests conducted *in situ* in substratum sand and point bar sands were corrected to an equivalent blow count, $(N_1)_{60}$, at a unit effective overburden pressure of 1 ton/ft^2 (1 kg/cm^2). The relative density was computed using the correlation between relative density and $(N_1)_{60}$ given in Skempton.[11] USACE engineering documents specified a minimum relative density of 85 per cent for the compacted sand backfill. The relative densities of the sand deposits were then used to estimate the hyperbolic stress–strain parameters using the data given in Duncan *et al.*[10] and Clough and Duncan.[4] The hyperbolic stress–strain parameters for the compacted clay backfill and backswamp deposit were estimated using correlations between engineering parameters determined in conventional index and strength tests (from the original laboratory testing program) and test results on similar types

of soils that are given in Duncan *et al.*[10] and Clough and Duncan.[4] The material properties and hyperbolic parameters assigned to the soil foundation, soil backfill, and soil berm are given in Ebeling *et al.*[2] and Ebeling and Mosher.[12]

4.3.2. Interface properties. Similarly, no specific tests were performed to define the hyperbolic shear stress-relative displacement relationship for the interface element used in SOILSTRUCT. The interface elements are used to describe the interface behaviour between the concrete lock and the foundation soil strata and between the lock and the backfill. By correlating the basic soil properties defined from the original testing program with soil-to-concrete interface direct shear tests conducted by Clough and Duncan[4] and Peterson, *et al.*,[13] the hyperbolic parameters for the model were established. The parameters assigned to the soil-to-lock interface regions are given in Ebeling *et al.*[2] and Ebeling and Mosher.[12] The use and performance of interface elements in the SSI analyses of Red River Lock No. 1 is discussed in Appendix II.

4.3.3. Reinforcement properties. The initial layout of reinforcement within the soil berm shown in Figure 5 assumed a polymer reinforcement with the following properties: (1) an allowable strength of the reinforcement of 3800 lb per lin ft of berm (57 kN per lin m of berm), and (2) a long-term tensile modulus of 50,000 lb per lin ft of berm (750 kN per lin m of berm), where the tensile modulus is the product of the long-term Young's modulus for the reinforcement and the cross-sectional area of the reinforcement per linear foot of berm. The long-term (120 yr) tensile modulus was computed from isochronous tension–strain curves at two per cent strain, as measured in long-term creep tests conducted on polymer reinforcement in the laboratory, at a constant temperature of 55°F.

4.4. Calibration studies of the finite element model of Red River Lock No. 1

The first phase of the soil–structure interaction study had as its objective the development of a finite element model and comparison of the results with instrumentation measurements for four extreme load cases (end of construction, low pool, high pool, and high pool with siltation). The results of these calibration studies at the instrumented lock monolith L-10 are discussed in detail by Ebeling *et al.*[2] and Ebeling and Mosher.[12] The results show that with the limited amount of data on soil properties and limited instrumentation readings, important aspects of lock performance from initial construction through major flood events, including siltation, were reasonably predicted using the finite element model of lock monolith L-10 in conjunction with the backfill placement method of analysis using SOILSTRUCT. It was likewise concluded that the predictions of future performance could be modelled accurately. The finite element mesh used in the calibration studies was extended to include the reinforced soil berm. The resulting mesh is shown in Figures 4 and 5.

5. BERM CONSTRUCTION AND FOUR OPERATIONAL EVENTS

The berm-to-lock interaction analyses described in this paper involve a series of incremental, non-linear finite element analyses simulating the stages of berm construction, raising of the upper and lower pool levels (above and below the dam), silt loading, and subsequent lowering of the pool levels. This series of analyses has seven distinct stages, which are listed in Table I and depicted in Figure 6. The initial stage, prior to berm construction, at the cross section for lock

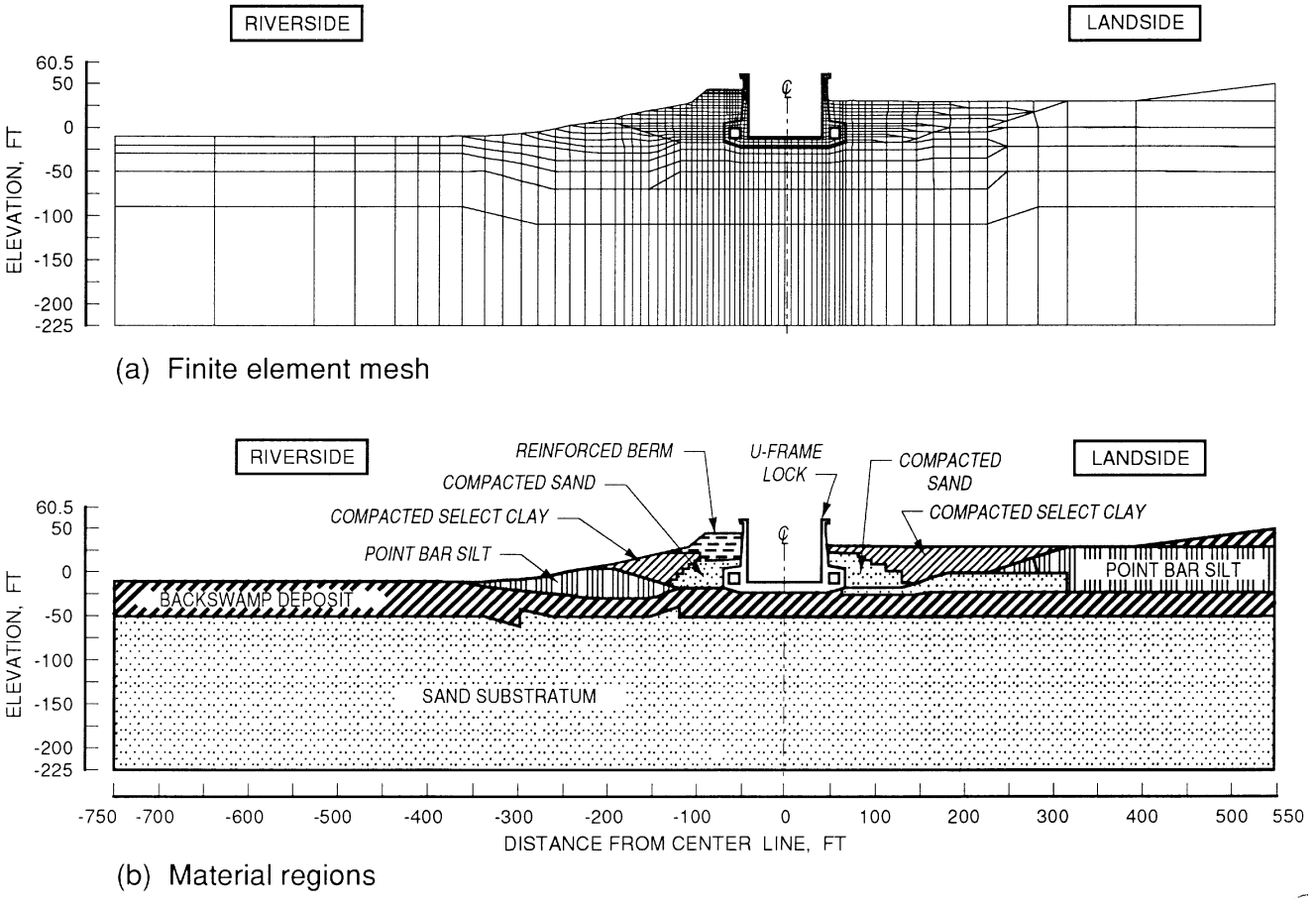

Figure 4. Finite element mesh and corresponding material regions after lock construction of reinforced berm (1 ft = 0·305 m)

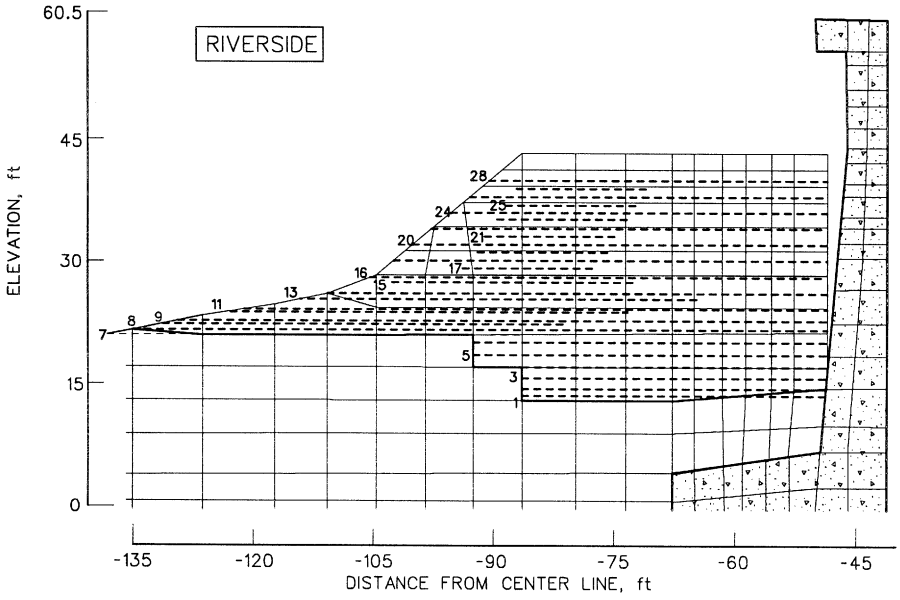

Figure 5. Layout of 28 layers of reinforcement within the riverside berm region of the mesh (1 ft = 0·305 m)

Table I. Stages of finite element analyses

Description of load case	Symbol	Elevation			
		Water table (ft)	River (ft)	Pool in lock (ft)	Riverside silt (ft)
Initial state	I	11	11	11	—
Excavate for riverside reinforced berm	E	11	11	11	—
Construct reinforced berm	1	11	11	11	—
Submergence of reinforced berm	2	60·5	60·5	60·5	—
Deposition of 10 ft of riverside silt on reinforced berm	3	60·5	60·5	60·5	55
Lowering river elevation and pool in lock	4	4	4	40	55
Lowering pool in lock	5	4	4	4	55

(1 ft = 0·305 m)

monolith L-10 is labelled as I in Figure 6. Excavation and construction of the reinforced berm are expected to take place during the dry season at the lock. A lower pool at el 11 (3·35 m) is consistent with the construction requirements and is often encountered during the dry season at the lock. The initial stresses and displacements for the berm–lock interaction analyses were computed at an intermediate stage of the calibration study series of lock construction and backfill

placement (see Reference 2) in which the soil foundation and backfill were submerged below el 11 ft (3·35 m) and the pool in the lock was at el 11 ft (3·35 m).

The first series of analyses, labelled as E in Figure 6, models the partial excavation of the riverside backfill to el 13·5 ft (4·11 m) with the water table maintained at el 11 ft (3·35 m) below the base of the excavation. The deepest excavation occurred adjacent to the riverside lock wall where the backfill was lowered by 17·5 ft (5·33 m), from el 31 ft (9·45 m) to el 13·5 ft (4·11 m). The simulated excavation was done in the finite element analysis by use of SOILSTRUCT using four unload increments.

The next series of finite element analyses, labeled as 1 in Figure 6, models the construction of the reinforced berm (Figure 5) to el 45 ft (13·72 m) in ten increments using the backfill placement

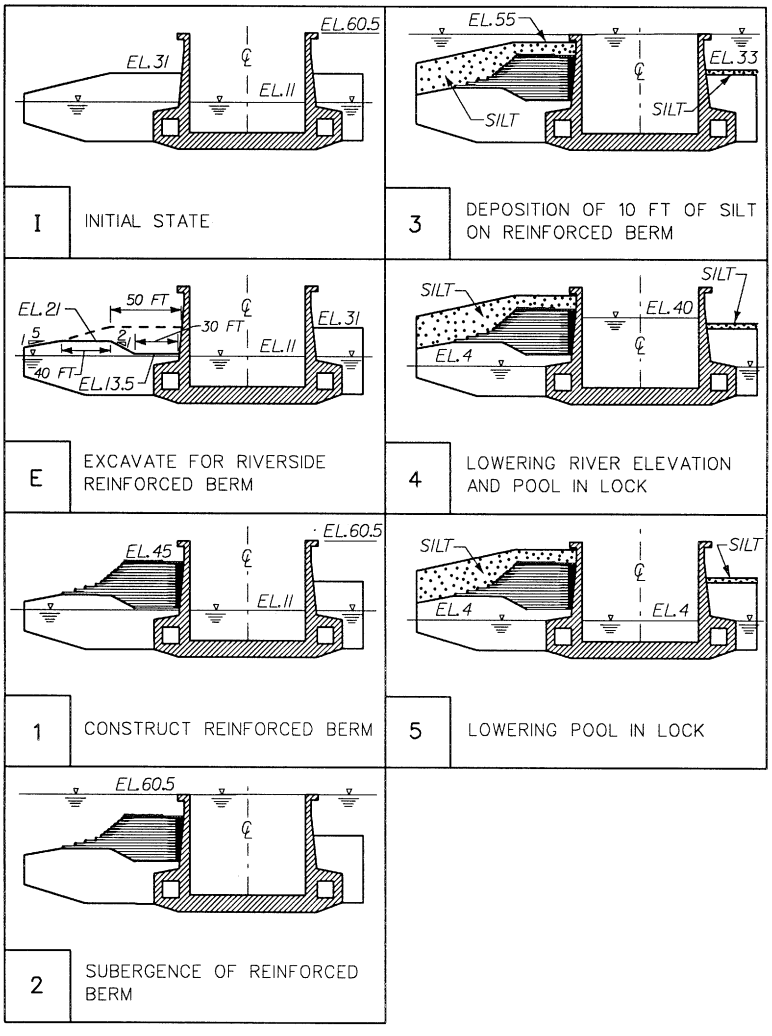

Figure 6. Load cases modelled in the finite element analyses (1 ft = 0·305 m)

method incorporated within SOILSTRUCT. The finite element mesh of the lock, backfill, foundation, and reinforced berm is shown in Figure 4(a). The mesh consists of 1152 two-dimensional elements (including 206 linear two-dimensional elements to model the lock), 56 interface elements between the soil and the lock, and 1257 nodes. The 31·5 ft tall (9·6 m tall) reinforced berm was modelled using 113 two-dimensional elements. A gap is included in the mesh between the lockside face of the reinforced berm and the stem wall to eliminate the transfer of earth pressures to the lock between els 13·5 and 45 ft (4·11 and 13·72 m).

The subsequent series of incremental analyses (labelled 2–5 in Table I and Figure 6) corresponds to the high pool [el 60·5 ft (18·44 m)] load case, high pool with riverside siltation to el 55 ft (16·76 m), lowering of river to el 4 ft (1·22 m) and lowering pool in lock to el 40 ft (12·19 m), and, lastly, lowering the pool in the lock to el 4 ft (1·22 m).

In all cases analysed drained conditions with effective stress soil properties were used. The critical loading condition of the lock by the berm was a fully consolidated, long-term condition for which effective stress parameters are appropriate. The undrained condition that existed during berm construction was shown to be stable by conventional equilibrium procedures. Moist unit weights were assigned to soils above the water table and buoyant unit weights were assigned to soils below the water table. Effective stresses were calculated within each soil element with changes in water table elevation through the application of consistent buoyancy forces applied to each soil element. Water pressures acting within the lock chamber and culverts, and against the base and the exterior culvert and stem walls were modelled as a boundary pressure.

5.1. Distribution of vertical effective stresses within the foundation

A critical point in the compressibility of soils is the preconsolidation pressure. Consolidation tests results indicated that for some soils comprising the Backswamp Deposit, settlements during virgin loading (when σ'_y exceeds p_c) can be up to ten times the settlements during reloading (when σ'_y is less than p_c) for a given change in stress. This factor of ten is typical of insensitive clays (Reference 14). The potential for the magnitude of settlement to be anticipated can be seen from a plot of the vertical effective stresses σ'_y versus depth compared to the values of preconsolidation pressure p_c. Values of σ'_y are computed at various stages of loading and unloading. The focus of our concern was the Backswamp Deposit because results of one-dimensional consolidation tests on samples recovered across the site and tests during the design of the lock showed the Backswamp Deposit to be far more compressible than the Sand Substratum (the strata are shown in Figure 4b) at the lock monolith L-10 section).

The variation in vertical effective stresses σ'_y computed within the soil foundation elements below the stem walls are shown in Figure 7 at the five stages of loading and unloading, labelled 1–5 in Table I and Figure 6. The two-dimensional nature of loading/unloading is evident when the values of σ'_y in Figures 7(b) and 7(c) are compared at any given elevation. Also plotted in Figure 7 is the range in p_c values on Backswamp Deposit soil samples. It is important to note that the soil samples were recovered from across the site. None were recovered below the riverside region at lock monolith L-10. Within the Backswamp Deposit below the riverside stem wall [between el -23 ft ($-7{\cdot}01$ m) and el -50 ft ($-15{\cdot}24$ m) at this lock section], the computed values of σ'_y approach the lower range in p_c values for two of the fourteen consolidation tests for load case 4 [river at el 4 f (1·22 m) and pool in lock at el 40 ft (12·19 m). Below the landside stem wall, all values of σ'_y within the Backswamp Deposit are less than the range in p_c values for all fourteen consolidation tests for all load cases.

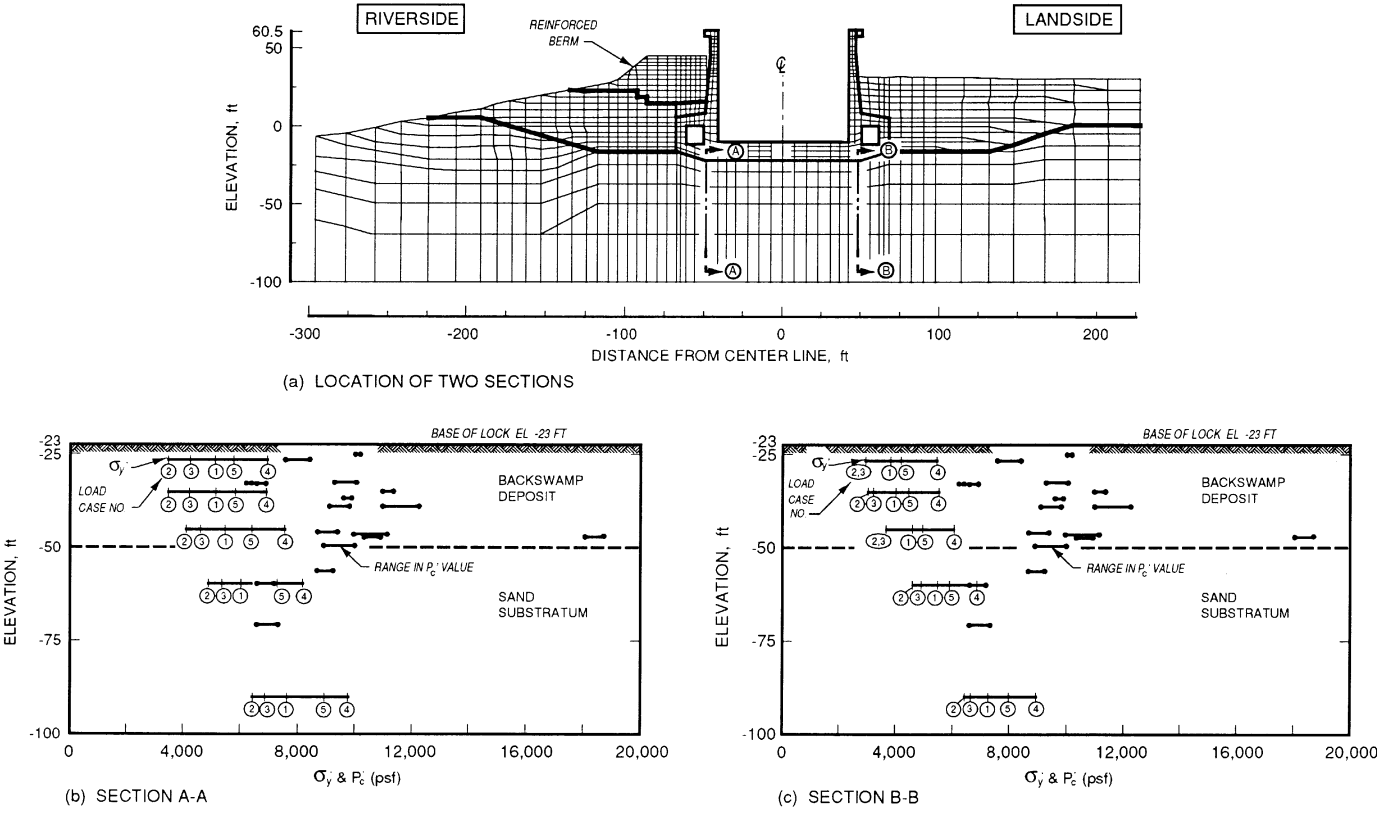

Figure 7. Two sections along which values of vertical effective stress are compared to range in preconsolidation pressure values within foundation (1 ft = 0·305 m, 1 psf = 47·88 Pa)

In summary, these results show that the loading is two dimensional, and that there may be a potential for virgin loading of the Backswamp Deposit below the riverside stem wall during load case 4. *This loading is greater than any experienced during the history of the project and would possibly involve the virgin loading in compression, a feature not encountered in the calibration studies.* Recall that the information made available for the study did not allow for a detailed calibration of the parameters assigned to the constitutive model. This lack of data was deemed acceptable in view of the results from the actual past structural performance.

The situation facing design engineers on the Red River project is similar to that experienced by Casagrande[15] in a study in which he was explaining the measured settlements on a large oil tank. In that study, the variations in induced pressures were computed within the foundation strata at two key locations, below the centre of the oil tank, and along the periphery. The changes in pressure were computed using the solution for circular area loaded uniformly with a pressure Δp and resting on an elastic-isotropic half space. Settlements were computed at the centre and below the periphery of the tank using conventional (one-dimensional) settlement theory with average compressibility characteristics of the foundation soils determined from a number of consolidation tests. Casagrande reported good agreement between computed settlements and observed settlements. An additional finding of relevance to the Red River berm study was that the ratio between settlements along the periphery and in the centre of a uniformly loaded area can vary within a wide range, dependent upon the magnitude of the induced pressures in relation to the preconsolidation of the subsoil. Casagrande attributed this result to the fact that regions of the foundation strata could be loading in virgin compression while other regions could be loading in recompression, or a combination thereof.

5.2. Distribution of horizontal and vertical movements of the lock and reinforced soil berm

Many of the design issues that could not be addressed during the initial reinforcement layout using limit equilibrium procedures are related to the movement of the reinforced berm relative to the movement of the lock during construction of the berm, and though major flood events, including siltation. Recall that the goal for this design is to provide 'pressure relief' from the silt by the berm being structurally independent from the riverside stem portion of the lock wall. The displacements of select points along the lock within the berm and foundation given in Figs 8–12 are computed *relative* to their position after excavation for the reinforced berm. These relative displacement correspond to the five load/unload cases listed in Table I and depicted in Figure 6.

Figure 8 shows that the greatest lateral movements with construction of the berm (case 1) occurred midheight along the inside vertical face of the berm, equal to 3·2 in (8·13 cm) and directed towards the riverside stem wall. The two-dimensional nature of loading is evident in this figure when the values of horizontal and vertical movements are compared across the lock.

Flooding of the site (case 2) to el 60·5 ft (18·44 m) reduces the relative settlement of the lock as shown in Figure 9, as compared to values shown in Figure 8. The upward movements of both the lock and the berm are attributed to the effect of buoyancy as a result of their submergence. The lateral movement midheight along the inside vertical face of the berm increased over the dry berm case 1 values by 0·4 in (1·02 cm) towards the stem wall.

Riverside siltation (case 3) to el 5 ft (16·76 m) increases the relative settlement of the riverside stem wall, shown in Figure 10, by about 0·3 in (0·76 cm) compared to values computed after flooding (Figure 9). The lateral movement midheight along the inside vertical faces of the berm increased by 0·5 in (1·27 cm) to 4·1 in (10·41 cm) towards the stem wall.

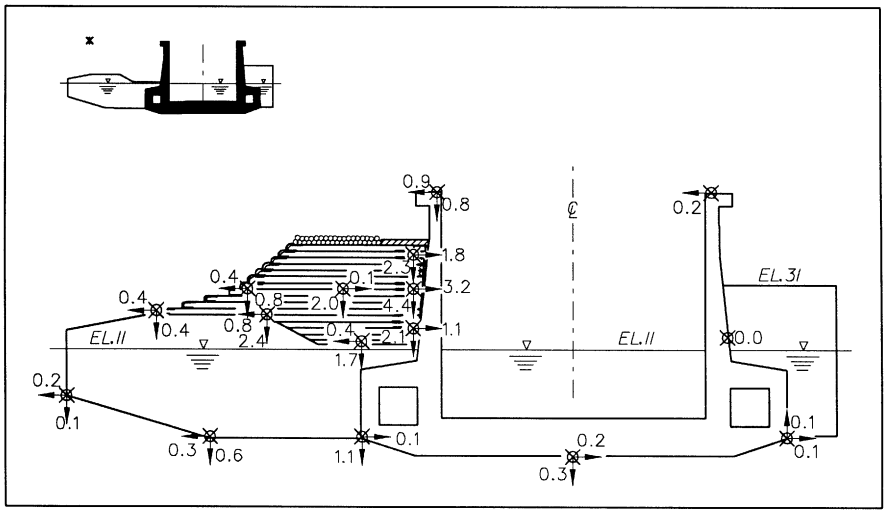

* DISPLACEMENTS OF POINTS ARE RELATIVE TO THEIR POSITION AFTER EXCAVATION FOR REINFORCED BERM, IN INCHES.

Figure 8. Relative displacements of lock, berm, and foundation after construction of reinforced berm (1 in = 2·54 cm)

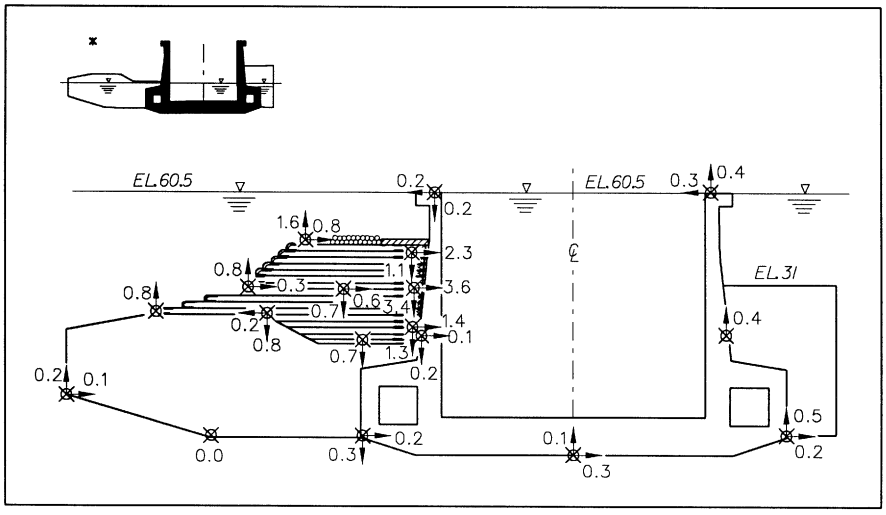

* DISPLACEMENTS OF POINTS ARE RELATIVE TO THEIR POSITION AFTER EXCAVATION FOR REINFORCED BERM, IN INCHES.

Figure 9. Relative displacements of lock, berm, and foundation after submergence of reinforced berm (1 in = 2·54 cm)

Lowering of the pool in the lock (and river upstream of the dam) to el 40 ft (12·19 m) and lowering of the river (downstream of the dam) to el 4 ft (1·22 m) in case 4 increases the relative settlement of the riverside stem wall (Figure 11) to 2·3 in (5·84 cm). The differential settlement equals 1·9 in (4·83 cm) across the base of the lock. The greatest lateral movement computed along

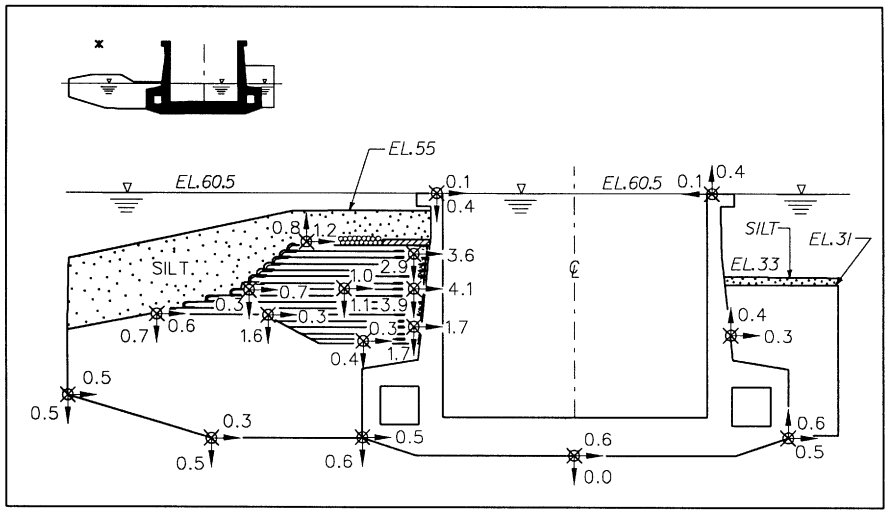

* DISPLACEMENTS OF POINTS ARE RELATIVE TO THEIR POSITION AFTER EXCAVATION FOR REINFORCED BERM, IN INCHES.

Figure 10. Relative displacement of lock, berm, and foundation after reverside siltation of reinforced berm to el 55 ft (1 in = 2·54 cm)

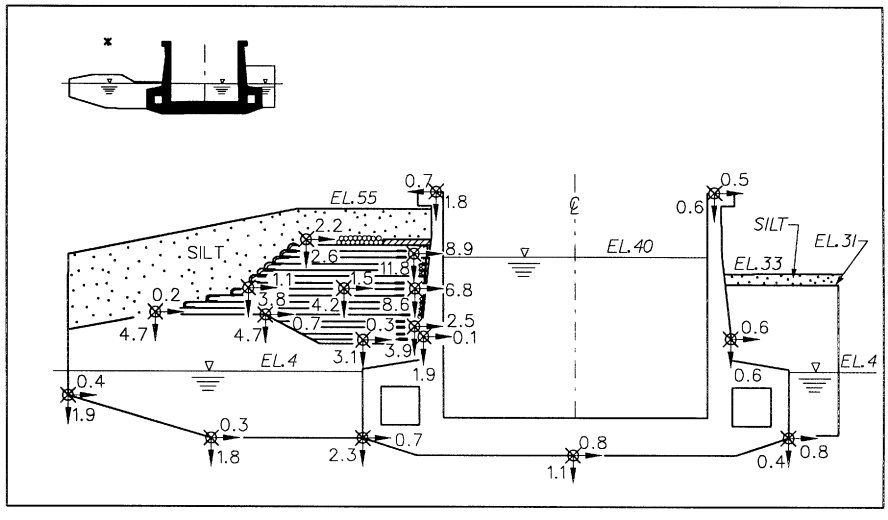

* DISPLACEMENTS OF POINTS ARE RELATIVE TO THEIR POSITION AFTER EXCAVATION FOR REINFORCED BERM, IN INCHES.

Figure 11. Relative displacements of lock, berm, and foundation after lowering pool in lock to el 40 ft and river to el 4 ft (1 in = 2·54 cm)

the inside vertical face of the berm shifted from midheight to the top of the berm and equaled 8·9 in (22·61 cm). With lowering of the river and pool, the top of the riverside stem wall moved towards the berm by 0·8 in (2·03 cm) to a relative displacement of 0·7 in (1·78 cm).

Lowering of the pool in the lock (case 5) to el 4 ft (1·22 m) with the river maintained at el 4 ft (1·22 m) decreased the relative settlement of the riverside stem wall (Figure 12) to 1·8 in (4·57 cm). The greatest lateral movement at the top of the inside vertical face of the berm equaled 8.8 in (22·35 cm) towards the stem wall.

In summary, the largest relative displacements were computed after riverside siltation and lowering of the river to el 4 ft (1·22 m) and pool in lock to el 40 ft (12·19 m). In load case 4, the greatest closure of 'the gap' between the reinforced berm and the lock wall was computed to be 9·3 in (23·62 cm) at el 41 ft (12·5 m). These displacement calculations proved to be critical in the evaluation of the adequacy of the reinforcement layout and the assessment of filler materials to be placed in the gap to eliminate the potential for siltation within the gap while preserving the structural independence of the berm from the riverside stem wall.

5.3. Mobilized shear resistance within the soil comprising the reinforced berm

Figure 13 shows the variation in the mobilized shear resistance within the soil after construction of the reinforced berm (case 1). The formulation used in SOILSTRUCT defines the mobilized shear resistance SL as equal to the deviator stress $(\sigma_1 - \sigma_3)$ divided by the deviator stress at failure $(\sigma_1 - \sigma_3)_{\text{failure}}$ computed in each soil element and at each stage of loading/unloading. The deviator stress at failure is computed using the Mohr–Coulomb failure criteria.[3] SL will range in value from 0·0, corresponding to no mobilization of shear strength, to fully mobilized shear

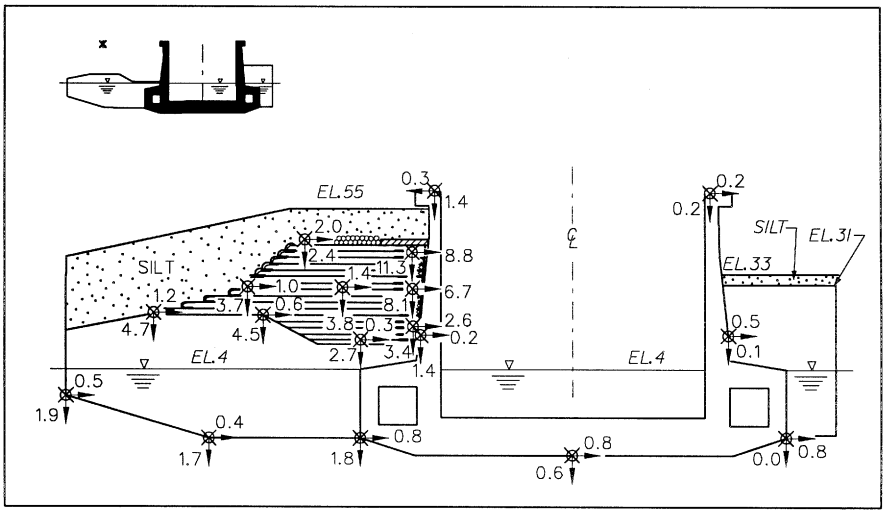

* DISPLACEMENTS OF POINTS ARE RELATIVE TO THEIR POSITION AFTER EXCAVATION FOR REINFORCED BERM, IN INCHES.

Figure 12. Relative displacements of lock, berm, and foundation after lowering pool in lock to et 4 ft and river at el 4 ft (1 in = 2·54 cm)

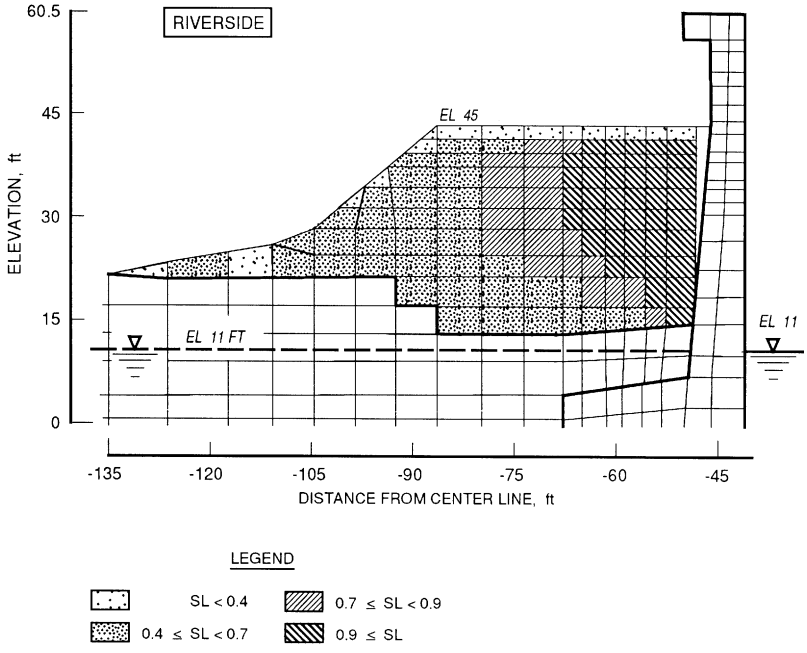

Figure 13. Variation in mobilized shear strength within the reinforced berm after construction of the berm (1 ft = 0·305 m)

strength with SL = 1·0. The soil comprising the side of the berm with the vertical face exhibited a highest level of mobilized shear when compared with the centre and riverside regions of the reinforced soil berm. In fact, this region fully mobilized the shear resistance and resembled the active wedge of soil that is assumed in classical Rankine limiting equilibrium analysis.

Figure 14 shows the variation in the mobilized shear resistance within the soil for case 5 after riverside siltation and lowering of the pool in the lock and lowering of the river to el 4 ft (1·22 m). Comparison of the distribution of SL values within the soil elements in Figures 13 and 14 shows that the region of fully mobilized shear resistance expanded to include the upper portion of the central region of the reinforced berm. With the computed values of SL $< 0{\cdot}9$ within the riverside region of the berm, the silt within the riverside channel provides more confinement than induced shear. The SL results shown in Figure 14 were nearly constant throughout the course of lowering the pool in the lock from el 40 ft (12·19) in case 4 to el 4 ft (1·22 m) in case 5.

In summary, the non-linear deformation analyses show that a 'wedge' developed behind the vertical face region of the reinforced soil berm. *The 'active' condition assumed in earth pressure theory is consistent with the results of these non-linear finite element analyses.* After riverside siltation and lowering of the pool in the lock and lowering of the river to el 4 ft (1·22 m), the silt within the riverside channel provides more confinement than shear within the reverside region of the berm.

5.4. Distribution of tensile forces within the layers of reinforcement

When using limit equilibrium procedures in design, a distribution of tensile forces within the layers are assumed during the layout of the reinforcement. The non-linear deformation analysis

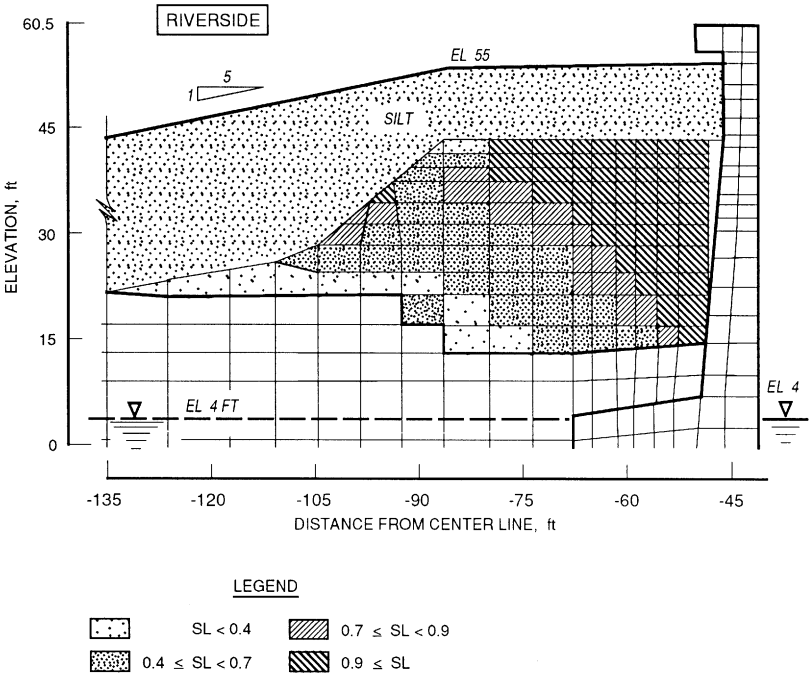

Figure 14. Variation in mobilized shear strength within the reinforced berm with riverside silt, pool in lock and lower pool at el 4 ft (1 ft = 0·305 m)

provides the designer the opportunity to compute the actual distribution of tensile forces throughout the layers of reinforcement.

Figure 15 shows the variation in tensile forces within each of the layers of reinforcement after construction of the reinforced berm (case 1). The range in tensile force is reported for all layers contained within each of the soil elements comprising the berm. The individual layers of reinforcement are not depicted in Figure 15 because of the density of reinforcement throughout the mesh. The largest tensile forces, less than 1200 lb per lin ft of berm (18 kN per lin m of berm), are computed within the layers of reinforcement adjacent to the lower inside vertical face of the reinforced berm. As expected, these forces are less than their allowable strength [3800 lb per lin ft (57 kN per lin m)], since the construction of the soil berm is not the most severe load case. The tensile forces within each layer of reinforcement are shown to diminish in magnitude with distance away from the vertical face and into the depths of the berm.

Figure 16 shows the variation in tensile forces within each of the layers of reinforcement within each soil element for case 5 after riverside siltation and lowering of the pool in the lock and lowering of the river to el 4 ft (1·22 m). The largest tensile forces, less than 2600 lb per lin ft of berm (39 kN per lin m of berm), are computed within the layers of reinforcement adjacent to the upper inside vertical face of the reinforced berm. The tensile forces are less than their allowable strength [3800 lb per lin ft (57 kN per lin m)]. The tensile forces shown in Figure 16 were nearly constant throughout the course of lowering of the pool in the lock from el 40 ft (12·19) in case 4 to el 4 ft (1·22 m) in case 5.

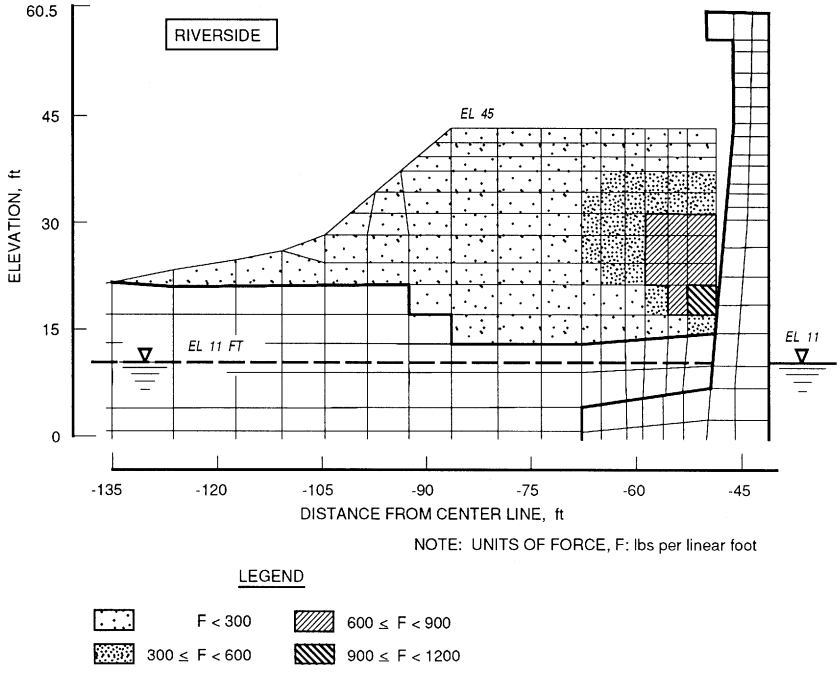

Figure 15. Variation in reinforcement force within the reinforced berm after construction of the berm (1 ft = 0·305 m, 1 lb per linear foot = 0·015 kN per linear meter)

In summary, the greatest values of tensile forces within layers of reinforcement and the greatest values of lateral deformations were computed after siltation and lowering of the pool in the lock and lowering of the river (cases 4 and 5). These values occurred in the region at the top of the vertical face of the reinforced soil berm. *The distribution of* SL *and tensile force was as expected for the active condition on the vertical face but not for the deep-seated condition shown in Figure* 3. Based on mobilized shear resistance, reinforcement forces, and movements, the analysis gave no evidence of a potential deep-seated slope movement against which the reinforcement was designed.

5.5. Distribution of moments within the lock

Figure 17 shows the distribution of the factored equivalent moments (i.e. the demand) using solid circles as symbols computed from the stress distributions across each of the finite elements comprising the lock, along with the distribution of design moments (i.e. the capacity). The factored equivalent moments were computed in two stages at each imaginary section along each structural member comprising the U-frame lock. First, the stress distribution normal to a plane, defined by a vector along the neutral axis, was converted to an equivalent-moment about the neutral axis using the flexure formula. The computed equivalent moment was then multiplied by a factor of 2·21. This factor reflects the extreme load case and is equal to the product of 1·3, the factor applied to hydraulic structure, times 1·7, the factor applied to live loads. Figure 17 shows

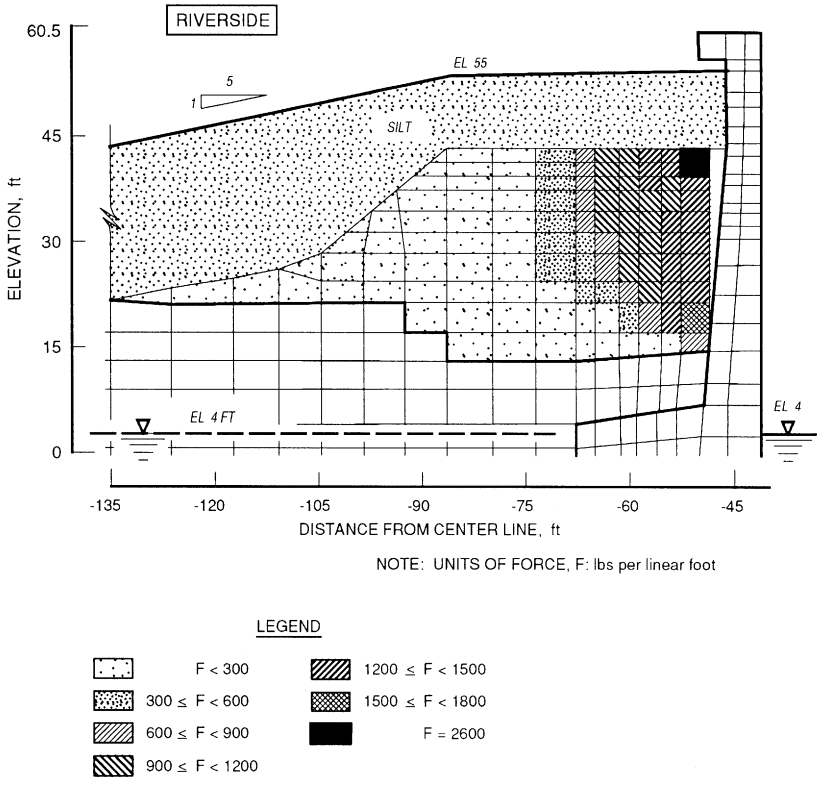

Figure 16. Variation in reinforcement force within the reinforced berm with reverside silt, pool in lock and lower pool at el 4 ft (1 ft = 0·305 m, 1 lb per linear foot = 0·015 kN per linear meter)

that at lock monolith L-10 for load case 4 [river at el 4 ft (1·22) and pool in lock at el 40 ft (12·19 m)], the lock is not in danger of failure in flexure.

Lowering of the pool in the lock (case 5) to el 4 ft (1·22 m) with the river maintained at el 4 ft (1·22 m) increases the factored equivalent moments in the top of the riverside culvert, as shown in Figure 18, compared to those moments computed in this structural member for load case 4 (Figure 17). The non-linear deformation analyses showed a unique situation. The higher moment demand on this structural member is due to the loadings imposed by a change in pool elevation *within* the lock chamber while the riverside berm and silt load remained unchanged. The flexural demand on the chamber floor also increased with the lowering of the pool in the lock. However, neither these two members nor all other structural members comprising the lock structure are in danger of failure in flexure.

In summary, none of the structural members comprising the lock structure are in danger of failure in flexural during either construction of the berm or during raising of the upper and lower pool levels (above and below the dam), silt loading, and subsequent lowering of the pool levels. The results shown in Figures 17 and 18 illustrate the sometimes complex soil-to-structure-to-foundation interactions that can occur during changes in operating conditions at a soil-founded U-frame lock. *A non-linear deformation analysis that completely addresses all aspect of soil–structure interaction is needed to understand these interactions.*

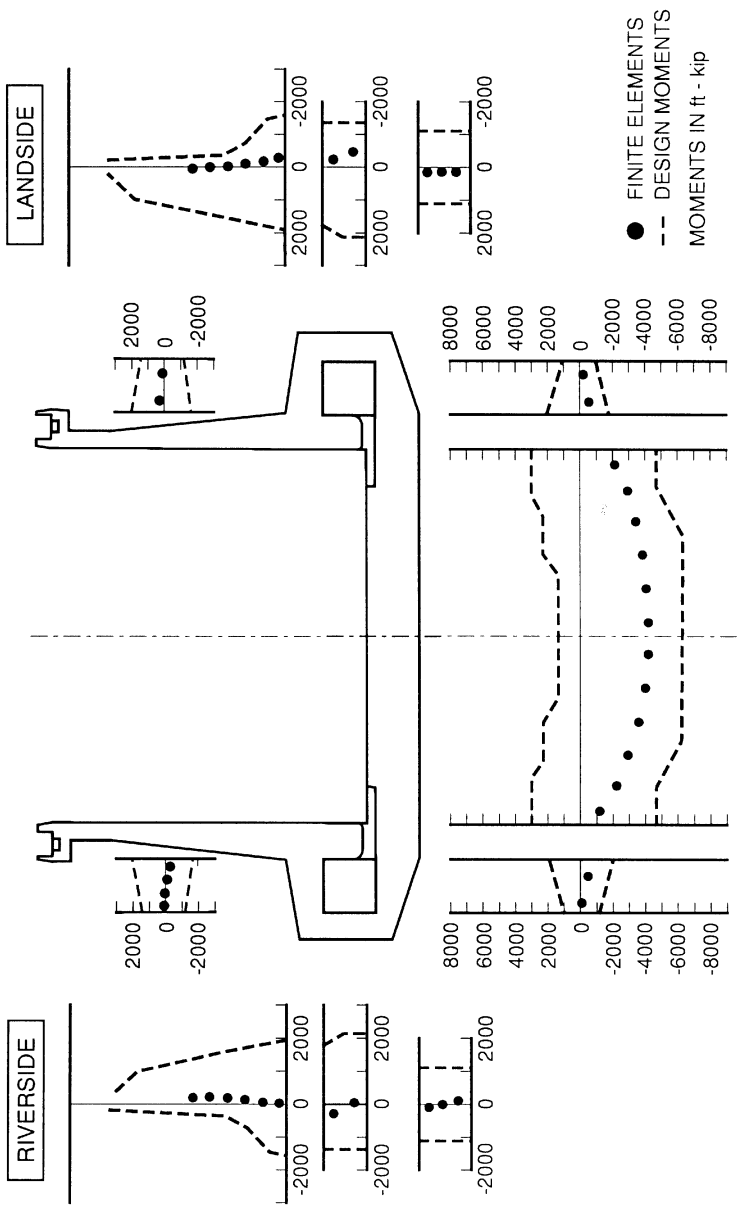

Figure 17. Distribution of factored moments and design moment capacity—pool in lock at el 40 ft and river at el 4 ft (1 ft-kip = 1·3558 m-kN)

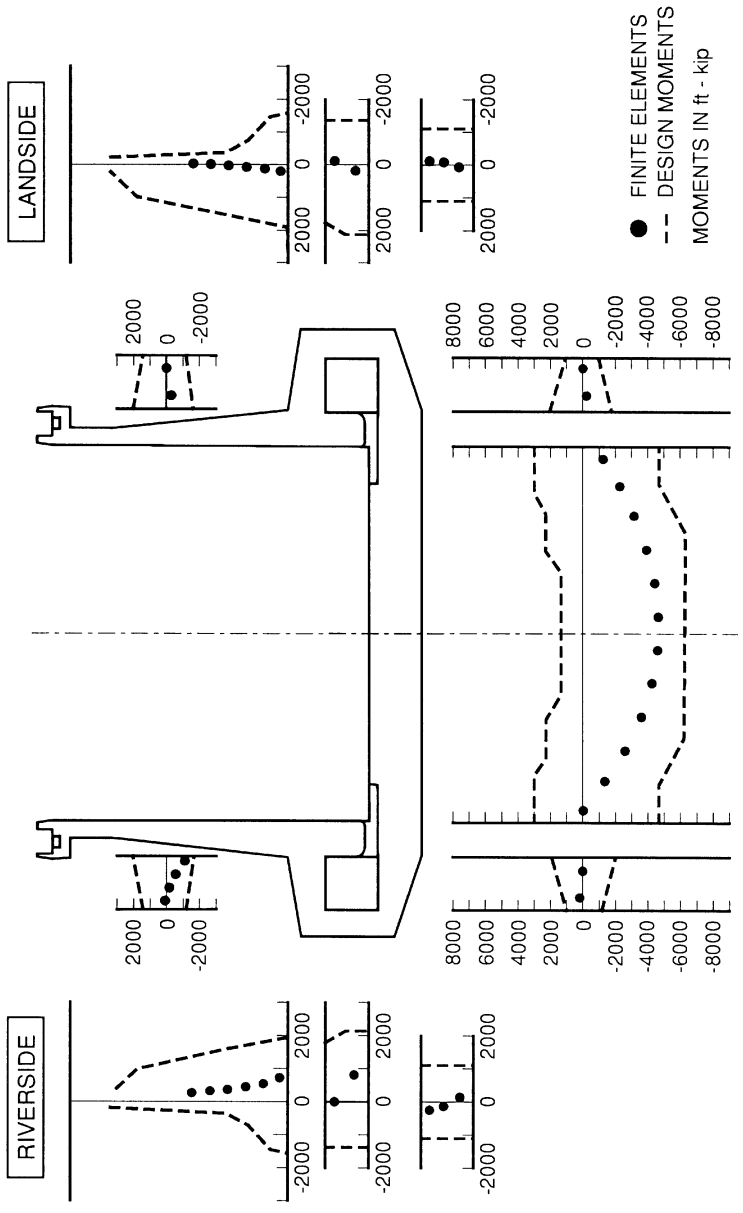

Figure 18. Distribution of factored moments and design moment capcity—pool in lock at el 4 ft and river at el 4 ft (1 ft-kip = 1·3558 m-kN)

6. LIMIT EQUILIBRIUM DESIGN PROCEDURES

The philosophy behind the layout design using limit equilibrium procedures is that the reinforcement provides the additional resistance to the soil to bring the factor of safety to an acceptable value. The limit equilibrium procedure is simple and provides a rational design approach when the factor of safety is less than one. However, for cases such as Red River lock in which the factor of safety is greater than one, the limit equilibrium procedure fails because the force in the reinforcement depends on the reinforcement stiffness relative to that of the soil. There is no guarantee that the reinforcement will mobilize enough force to actually 'relieve' the soil of significant stress. Two results of the analyses presented in the previous sections bear this out. First, fabric forces near the vertical face adjacent to the lock wall, where a fully developed active wedge was formed, displayed a pattern consisent with the active conditions (Figure 13 and 14). Fabric forces were those needed to maintain equilibrium in the fully plasticized soil. Second, neither the force distribution in the reinforcement (Figure 15 and 16) nor the displacement pattern in the berm–foundation system (Figures 8–12) suggested that deep-seated movement was a major factor. For any deformation mechanism giving rise to an unreinforced (computed) factor of safety less than one, the minimum reinforcement forces will be what is needed to bring the system into equilibrium. In this case, all of the reserve rests in the reinforcement, and the 'factor of safety' is the force developed versus the strength of the reinforcement. Importantly, the reinforcement forces can be reliably predicted with limit-equilibrium methods if the reinforcement stiffness is not too great. When the reinforcement stiffness is high, limit equilibrium methods may actually underestimate reinforcement forces.

When the factor of safety is greater than one, the load sharing capacity depends on the reinforcement stiffness, which is seldom great enough to make the expected contribution to the factor of safety. Limit equilibrium methods do not provide a means to compute reinforcement forces because the system is highly statistically indeterminate. The effectiveness of the reinforcement depends on factors such as stiffness and placement which are unaccounted for in limit equilibrium, computations. Unless the failure mechanism is fully delineated, the only way to properly assess the suitability of a reinforcement layout is to perform a non-linear deformation analysis that accounts for the interaction between the reinforcement and the soil. A displacement analysis is needed even when displacements per se are not of interest.

Further, a traditional design for the lock wall to determine moments in the wall would require empirical pressure diagrams appropriate for each of the many loading cases. An illustrated by the unique nature of the interactions, a single empirically based pressure diagram cannot exist. Experience with lock structures dating back to the analysis of Port Allen and Old River lock and dams by Clough and Duncan[4] shows that an accurate prediction of structural performance requires a detailed representation of the *foundation soil*(*s*), *the construction sequence*, *and the structural stiffness.*

7. CONCLUSIONS

1. Starting with a finite element model of lock monolith L-10 that was validated against instrumentation measurements at the end of lock construction and for three widely different operational load cases, a model of the proposed reinforced soil berm was added. Important aspects of lock and berm performance from construction of the berm through major flood events, including siltation, were predicted using the backfill placement method of analysis procedure

incorporated within SOILSTRUCT. Insight into the soil–structure–foundation interactions among the lock, the backfill, the reinforced berm, and foundation soil strata along with soil-geoinclusion interactions between the reinforcement and the soil comprising the reinforced berm were gained through use of a nonlinear deformation analysis.

2. The results of this study show that conventional limit equilibrium analysis, one-dimensional settlement analysis used in traditional geotechnical design, and empirical pressure diagrams are deficient for this problem. SOILSTRUCT represents the next level of complexity that is a balance between modelling realism and simplicity. Despite its well known deficiencies, the hyperbolic model rightly retains popularity for the type of problem described here because it captures key elements of design.

3. Limit equilibrium methods indicated the potential the potential for a deep-seated failure for which the deformation analysis gave no evidence. Further, the deformation analysis showed the need to increase reinforcement within an active wedge along the vertical face of the berm for which a limit equilibrium analysis was not done. We hasten to add, that our experience shows that when a deformation analysis indicates that a failure mechanism can develop, the factor of safety computed by use of a limit equilibrium analysis is approximately one (or less). The problem is that for a complicated structure, it is often difficult to discern the failure mechanism(s) to which the limit equilibrium analysis should be applied.

4. Whenever using one-dimensional settlement analysis or detailed SSI, the induced stress level should be compared to the past consolidation stress.

5. Consideration of the deformations which occur during various stages of lock operation is an essential part of the reinforced soil berm design given the sometimes complex interactions that occur between the lock, the backfill, the reinforced berm, and foundation soil strata, which is further compounded by the soil-geoinclusion interactions between the reinforcement and the soil comprising the reinforced berm.

ACKNOWLEDGMENTS

The assistance of Messrs. Kevin Abraham, C. C. Hamby, Ed Schilling, Sam Stacy, George Sills, and Wayne Forrest during this study is gratefully acknowledged. Permission was granted by the Chief of Engineers to publish this information.

APPENDIX I: DERIVATION OF EMBEDDED ELEMENT STIFFNESS

The embedded element formulation applies a common method of constraint application to connect dense arrays of geotextile reinforcement layers onto solid finite elements without increasing the number of displacements degrees of freedom. The method provides an alternative to the typical method for analysing geotextile reinforcement by finite elements whereby tensile elements are placed between solid element, possibly sandwiched between slip elements. The method is restricted to the case where slip between soil and geotextile is of minimum importance (e.g. densely spaced grids). In this appendix the finite element formulation is described and analysis of results is illustrated by an example.

Embedded element concept

Embedded elements are tensile elements added in parallel (structurally) with solid elements to enhances stiffness without increasing the number of displacement degrees of freedom. Embedded elements are advantageous when the reinforcement spacing is such that soil-interface slip is not an issue yet the spacing is not sufficiently uniform to homogenize the stiffening effects of the reinforcement into the local constitutive response of the material. Analysis of dense geotextile reinforcement by use of finite element method requires complicated meshing to accommodate the closely spaced layers without creating large element aspect ratios. The number of displacement degrees of freedom is thus dictated by the geometry of the reinforcement grid rather than by what is needed for convergence to the solution. A method that separates the requirements for convergence from those of geometry to optimize the mesh design is preferred. Homogenization of reinforcing into the solids constitutive relationship assumes periodic spacing of the reinforcing layers which may not be true of the actual grid. Embedded elements are not restricted to any particular spacing or orientation or length.

In the finite element method, their is no restriction that elements acting in parallel must be connected to each other at nodal points. Rather, structural parallelism is achieved by assuming the two types of elements move compatibility. Embedded elements may or may not be placed at element boundaries, thus simplifying analyses when different reinforcement configurations are considered. The pattern of reinforcing layers can be changed without altering the mesh representing the solid elements. Changes in reinforcement layout requires changing only the descriptions of the individual reinforcement layers.

Embedded element formulation

An embedded element enhances the elastic component of the elemental stiffness by placing the tensile element in parallel (structurally) with the solid element. Given the solid elemental stiffness $\mathbf{K}^{\mathrm{e}}$ where

$$\mathbf{K}^{\mathrm{e}}\mathbf{d}^{\mathrm{e}} = \mathbf{f}^{\mathrm{e}} \tag{1}$$

and the stiffness of the reinforcement segment $\mathbf{K}^{\mathrm{r}}$ where

$$\mathbf{K}^{\mathrm{r}}\mathbf{d}^{\mathrm{r}} = \mathbf{f}^{\mathrm{r}} \tag{2}$$

the displacements of the reinforcement element are related to those of the solid element by the interpolation

$$\mathbf{d}^{\mathrm{r}} = \mathbf{N}(\xi)\mathbf{d}^{\mathrm{e}} \tag{3}$$

where ξ represents the local co-ordinates for the reinforcing segment. It follows from the principle of virtual work that the total element stiffness for an element with M embedded elements is given by

$$\mathbf{K}^{\mathrm{e}} + \sum_{i=1}^{M} \mathbf{N}_i^{\mathrm{T}}\mathbf{K}^{\mathrm{r}}\mathbf{N}_i \tag{4}$$

Equation (3) implies the nodes of the embedded element have the same displacement as the solid element. This constraint roughly creates compatibility between the embedded element and solid element and thus does not capture soil-reinforcement slip. Forces in the embedded element are

computed from equation (2) using equation (3) to determine $\mathbf{d}^r$. Reference 16 demonstrates the versatility of this type of formulation at the individual element level for three different modes of deformation where 'exact' solutions could be determined.

Preprocessing

As a preprocessing step, geotextile layers must be broken into segments that lie within each element. The process is performed in an element wise fashion. For each solid element, the table of reinforcement layers is searched to determine if any portion of any layer lies within the element. The portion of a layer that lies within an element is defined as a segment. The local co-ordinates of the nodes for the tensile element representing the segment are computed. The segments defined in the preprocessing are modelled as one-dimensional tension-only members whose stiffnesses are added to the elemental stiffness matrix via equation (4). The method is general and does not make any assumption about spacing or orientation of the layers. Because all operations are performed at the element level and because embedment element displacement boundary conditions coincide to those of the solid elements, modification to the routine are not required to account for problem-specific boundary conditions.

As a note on the search routine, it is difficult to distinguish which element a segment belongs to when the segment happens to lie on an element boundary. The difficulty arises because determination of whether a layer lies within an element depends on comparison of layer location and nodal co-ordinates, which are all real numbers. Due to round-off error a segment may be found to lie in the two adjacent elements (i.e. it is counted twice), none of the elements, or just one of the elements. To avoid complicating the search routine, layers that lie on element boundaries are offset from element boundaries by an amount that is insignificant relative to the problem dimensions but large relative to the precision of the computations.

Implementation

For the examples presented herein, the embedded elements were implemented using SOILSTRUCT,[3] a finite element program based on the QM5 formulation of Doherty *et al.*[17] The advantage of the QM5 is its superior representation of flexural modes of deformation that is achieved by adding internal degrees of freedom to allow a quadratic displacement distribution across the element (bubble function). To achieve optimal performance, the shear components of deformation are assumed to be constant. The interpolation is complete up to bi-linear terms but incomplete for quadratic terms. The question of interpolation order is complicated by the elimination of terms to achieve a constant shear. Therefore the practical meaning of compatibility between embedded and solid element is difficult to interpret for the QM5.

In contrast, the embedded reinforcement element is formed using a one-dimensional interpolation defined along its line of action. As a result, strict adherence to compatibility cannot be maintained between the two element types. It was found by computation for many test cases that a linear interpolation for the reinforcement elements gave accurate results for all spacings and orientations of reinforcing. The QM5 implementation with linear embedded elements amounts to assuming that the end nodes of the embedded element has the same displacements as the corresponding points within the solid element. Actual computations showed this method to work well. If the embedded elements are placed on element boundaries, compatibility is satisfied exactly. Reinforcing elements with quadratic interpolation gave erroneous results.

Soil-Geotextile slip

The inability for slip to occur between the soil and the geotextile reinforcement may cause concern because the no-slip assumption overestimates stiffness. Out experiences showed that for dense grids, slip is not of practical consequence. Where individual segments are isolated, and thus may be subject to large pull-out modes of deformation, reinforcing can be modelled in the conventional way by adjusting the mesh so that the individual layer lies between element boundaries; the individual layer can then be sandwiched between slip elements to allow slip deformation.

The potential for slip can be checked at the postprocessing level.[18] From a free-body diagram of the geotextile segment (Figure 19), it can be seen that the shear transfer between the geotextile reinforcement and soil is given by $\tau = (T_2 - T_1)/L$. In the limit, $\tau = \mathrm{d}T/\mathrm{d}L$. Thus, the shear transfer can be computed from the slope of the tensile stress versus length curve. The maximum shear transfer achievable is given by $\tau_{\max} = N/L \tan \phi$, where N is the total normal force acting on the geotextile and ϕ is the friction angle between the geotextile reinforcement and soil. If the applied shear stress is less than the inferface slip resistance, then the assumption of compatibility between soil and reinforcement is a reasonable approximation.

Example

The embedded element was used to examine the soil–structure interaction of a test wall loaded to failure[19] using the computer program SOILSTRUCT. Figure 20 shows the finite element representation of the wall. The wall–backfill system was constructed incrementally by placing backfill against the back wall as lagging was placed to create the front wall. After filling, a surcharge was imposed at the top of the wall in increments until large deformations were achieved. Measurements were made of front wall movement, settlement of the top surface, and reinforcement strain. All reinforcement layers were modelled as embedded layers. The horizontal shear stiffness of solid elements containing double layer fabric was reduced account for sliding along the fabric–fabric interface when the horizontal shear stress exceed the sliding resistance of that interface. Otherwise, all materials were assumed to be isotropic. The lagging wall consisted of solid timbers backed on the soil side of the wall with plywood. This composite wall had a very high axial stiffness but a very low bending stiffness. The wall was modelled with solid elements, with the elastic stiffness of the wall elements based on the flexural rigidity of the wall. Stiff compression-only bar elements were embedded vertically along the neutral axis to achieve the wall's high axial stiffness. The details of the wall test and attempts by fifteen research teams to predict results are available as symposium proceedings.[19] Analysis by use of the embedded element method includes both pre-test predictions[20] and a post-test assessment of lessons learned of the modelling exercise.[21] The post-test assessment indicated that errors in modelling resulted from inaccuracies in modelling structural details (errors due to differences between the pre-test descriptions and what was actually done during testing), not from deficiencies in the soil or reinforcement models.

The reinforced test wall example is interesting because the shear strength of the soil was at a fully mobilized active condition for most of the test. The principal elastic component of the system was the reinforcement which supplied the balancing forces needed to maintain the backfill in static equilibrium. The soil achieved the active state nearly as soon as it was placed and the wall supplied minimal bending resistance. The elements performed well. No numerical problems were

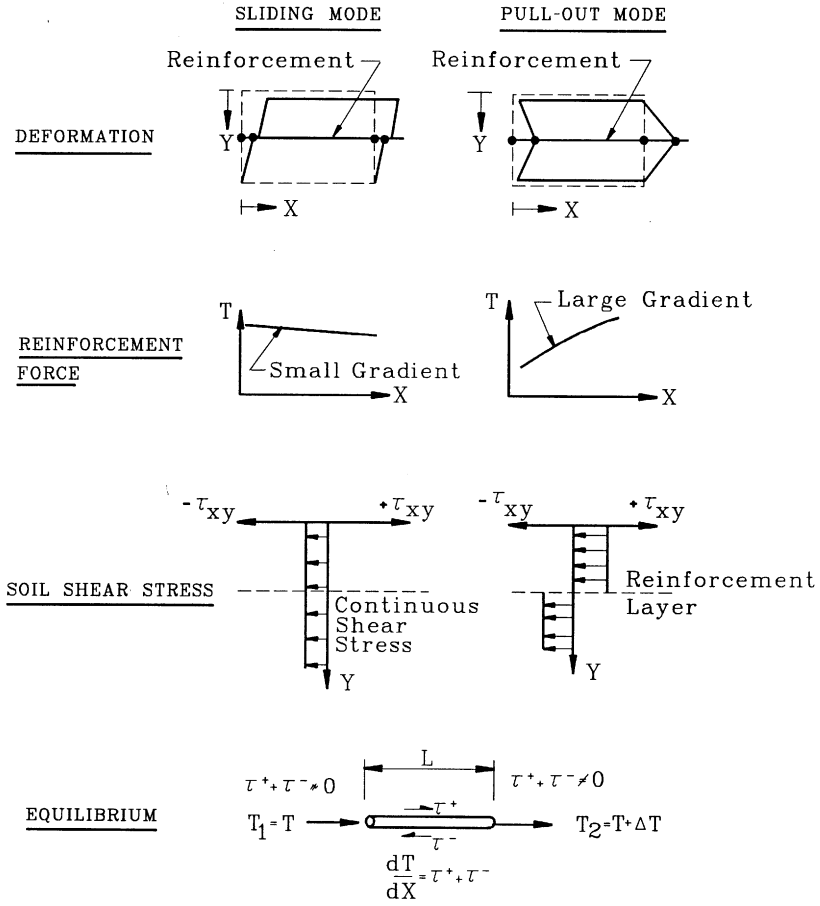

Figure 19. Slip and pullout modes of soil–reinforcement interaction[18]

encountered, and the distribution of reinforcement strain and displacements appeared to be reasonable, particularly in the post-test analysis in which structural behaviour was modelled better (see Figure 21). The check on the slip condition showed that none of the elements exceeded the pullout condition. That is, if interface elements had been used, *the slip condition would never have been activated.*

APPENDIX II: INTERPRETATION OF INTERFACE STRESSES

Interface elements are essential features in finite element analyses of soil–structure interactions of earth retaining structures. Interface elements are used to allow for *relative movement* between different material regions, such as between a soil backfill and support wall. Interface elements[22] were used between the concrete lock and the foundation soil strata and between the lock and the blackfill in this study. However, inclusion of interface elements in the finite element mesh does not in itself gurantee accurate results. It has been reported, e.g. in a study of pile-supported locks and

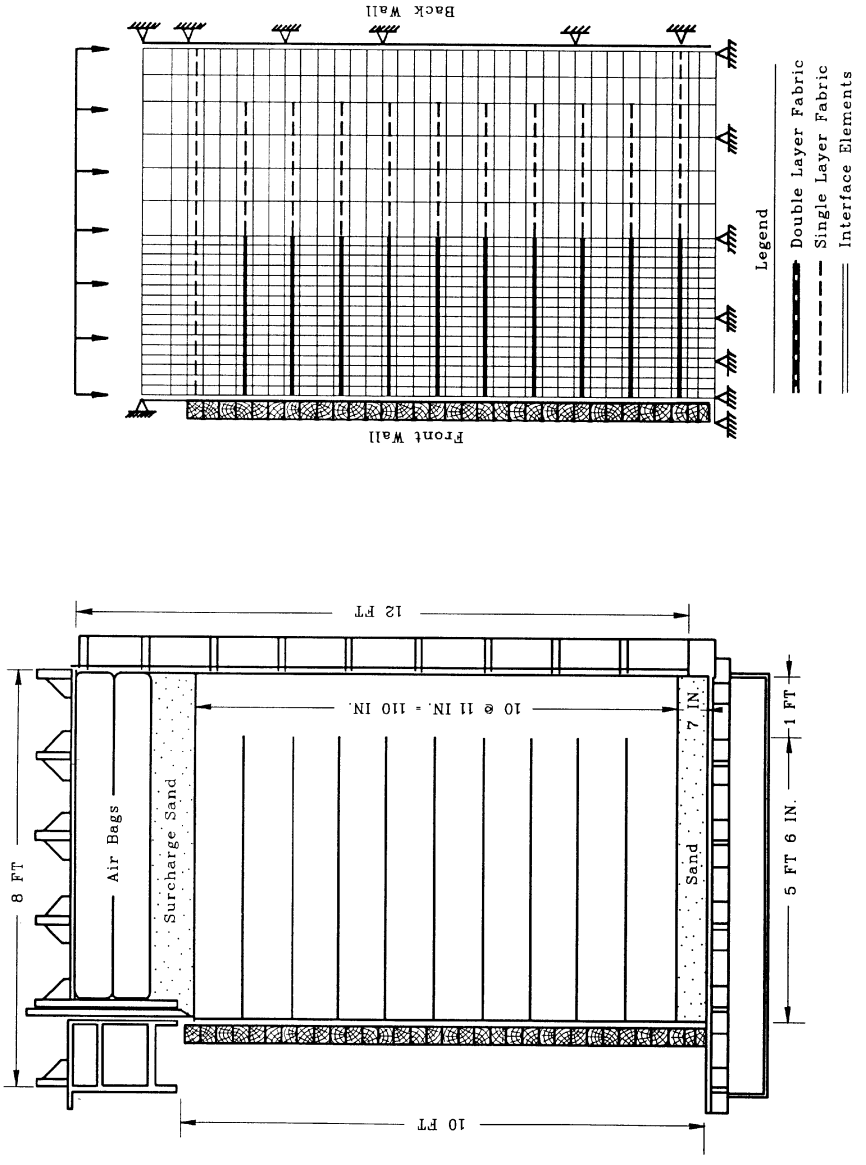

Figure 20. Denver wall configuration and finite element mesh used for analysis[20] (1 in = 2·54 cm, 1 ft = 0·305 m)

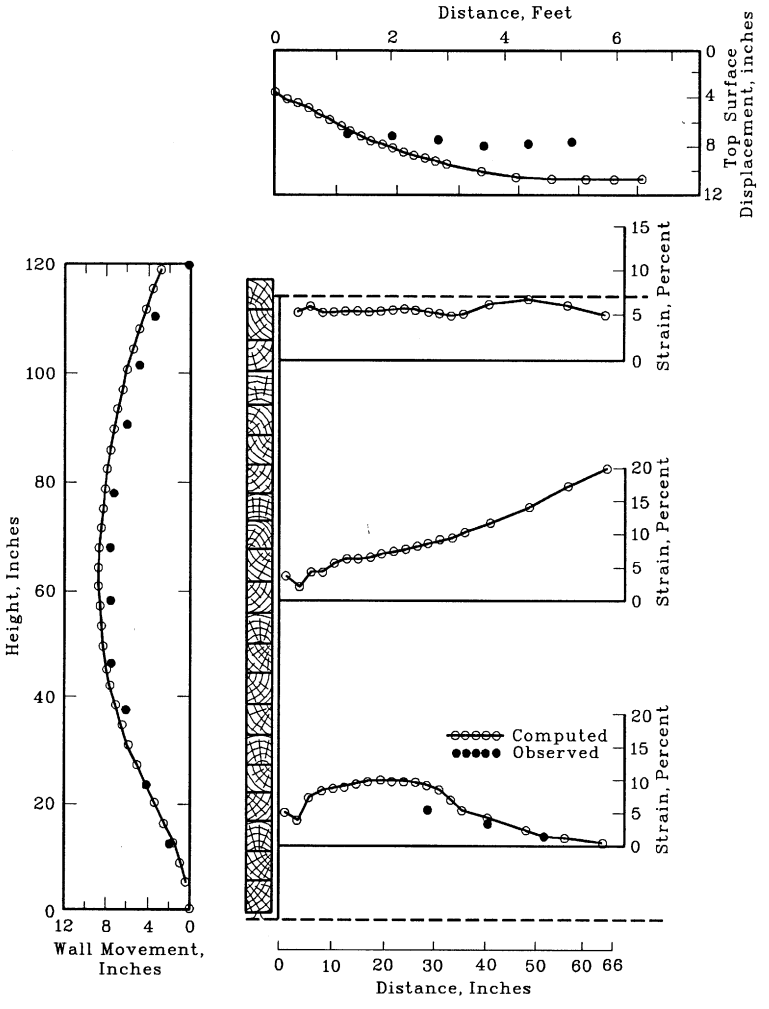

Figure 21. Postprediction versus observed behaviour for surcharge of 29 psi[21] (1 in = 2·54 cm, 1 psi = 6·0895 kPa). Some strain gage data missing because of loss of instrumentation at later stages of test

elsewhere,[23,24] that interface models may not provide realistic distribution of stresses and, thus, the lateral earth pressure on walls. This appendix describes some observations made regarding the use and performance of interface elements in the SSI analyses of Red River Lock No. 1.

It is standard practice in SSI analyses for engineers to check the performance of the finite element model at each stage of loading and unloading. One of these checks involves the comparison of pressures computed within interface elements with those pressures computed within adjacent soil elements along imaginary sections within the backfill. These imaginary sections are drawn parallel to the soil-to-lock interface, and the stresses computed within these soil elements are resolved normal to this imaginary section using Mohr's circle. Comparisons of this type were made throughout all stages of loading and unloading in the calibration study[12] and the assessment of the reinforced berm. An example of one comparison is shown in Figure 22,

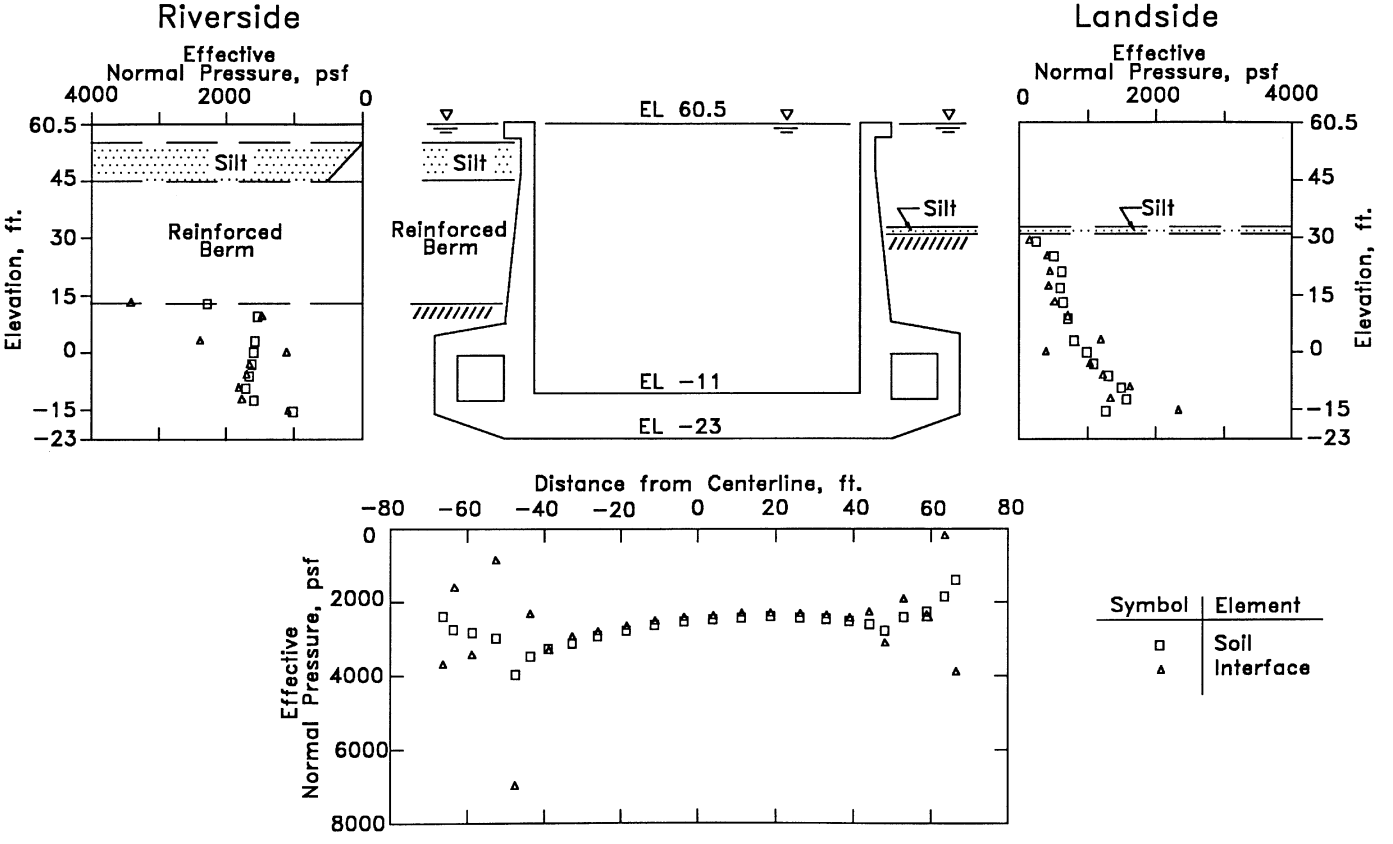

Figure 22. Effective normal pressures after riverside siltation to EL 55, river and pool in lock at el 60·5 (1 ft = 0·305 m, 1 psf = 47·88 pa)

corresponding to case 3 in Figure 5 of the main text. Case 3 is defined as the river and pool in lock at el 60·5 ft (18·44 m) with deposition of silt to el 55 ft (16·76 m) riverside of the lock. The effective normal pressures computed in the interface elments along the stem and culvert walls and along the lock base are shown in Figure 22 with the open triangle symbol. The effective normal pressures computed within the soil elements adjacent to the lock are also shown in Figure 22 with a solid square symbol. The effective normal base pressures along the base of the lock were computed using the effective stresses within the adjacent soil elements. These base pressures accounted for the difference in elevation between the base of the lock and the element centers [3·5 ft (1·07 m) on average].

Figure 22 shows general agreement between the distribution of effective normal pressures computed using interface elements with those distributions computed from stress data obtained from the adjacent soil elements. Some divergence is observed in the distribution of normal effective pressure within interface elements adjacent to the exterior corners of the curlvert when they are viewed on an individual element basis. However, there is a tendency for pairs of adjacent elements to compensate for each other's behaviour. One interface element may have high effective normal pressure while the other has low pressure. The authors have seen this type of interface behaviour in numerous SSI analyses and describe this phenomenon as 'racking' of interface elements. It is a phenomenon that is not unlike the singularity of stresses computed near abrupt geometry changes such as corners. The phenomenon is attributed to three factors, the displacement formulation to which the interface element is restricted, the variation in stiffnesses of the elements comprising this region of the mesh, and the geometry of the problem being modelled. Racking is observed at several of the corners in Figure 22. To reduce the extent of the region in which this phenomenon occurs a finer mesh with more interface elements is required. Because the racking effect is restricted to the pair of elements immediately adjacent to the corner, the length over which the effect occurs becomes small as the element becomes small.

The formulation of the Goodman–Taylor–Breeke[22] interface element satisfies equilibrium of forces at each node even when racking occurs. Thus, a consistent of set of forces is transferred between the soil and the lock through all nodes comprising the interface elements. So the primary question is with regards to the *distribution* of stresses *along* the backfill-to-stem wall, the backfill-to-culvert wall, and the foundation-to-lock base. To answer this question, a comparison of the data from interface elements with those from the adjacent soil elements is made. This comparison is particuraly useful when racking is observed. Figure 22 shows the distribution of pressures computed from soil elements to be smooth in the lock corner regions and the trend is to average the stresses within these regions where racking of interface elements is observed. To gain confidence in the results, the horizontal earth pressure coefficients were computed within each of the soil elements adjacent to the stem and culvert walls. These coefficients equal the horizontal effective earth pressures computed within the soil element divided by the effective overburden pressures at element centres. The plots for case 3 (Figure 141 in Reference 2) show logical and consistent trends with depth. Similar comparisons made for all other analyses show smooth distributions and consistent changes with loading and/or unloading. Thus, the smooth distribution of stresses shown in Figure 22 is interpreted as a testament to the adequacy of the size of the elements comprising the mesh.

After a careful evaluation of the checks described in this appendix, along with numerous other evaluations of the computed results (see Reference 2), the authors conclude that:

(1) The refinement of mesh and the number of interface elements are sufficient to produce accurate results,

(2) other than at the culvert corners, interface elements give generally consistent results with the adjacent soil elements,
(3) at culvert corners, the stresses computed within adjacent soil elements are more accurate than those computed within the *individual* interface elements,
(4) when the stresses computed within interface element are averaged along structural sections, the distributions are consistent with those distributions obtained from soil elements, and
(5) overall, the results of the complete soil–structure interaction analysis of Red River Lock No. 1 are accurate and capture the 'true' SSI of the lock-foundation-backfill.

REFERENCES

1. K. Terzaghi, 'Old earth-pressure theories and new test results', Engineering News Record, **85**(14), 632–637 (1920). Reprinted in *From Theory to Practice In Soil Mechanics, Sections from the Writings of Karl Terzaghi*, Wiley, New York, 1960, 108–113.
2. R. M.. Ebeling, R. L. Mosher, K. Abraham and J. F. Peters, 'Soil-structure interactions study of red river lock and dam no. 1 subjected to sediment loading'. *Technical Report ITL-93-3*, USAE Waterways Experiment Station, Vicksburg, MS, 1993.
3. R. M. Ebeling, J. F. Peters and G. W. Clough, 'Users guide for the incremental construction, soil-structure interaction program SOILSTRUCT', *Technical Report ITL-90-6, USAE* Waterways Experiment Station, Vicksburg, MS, 1992.
4. G. W. Clough and J. M. Duncan, 'Finite element analyses of port allen and old river locks', *Contract Report S-69-6*, USAE Waterways Experiment Station, Vicksburg, MS, 1969.
5. J. M. Duncan and G. W. Clough, 'Finite element analyses of port allen lock', *J. Soil Mech. Found. Div.*, **97**(SM8), 1053–1068 (1971).
6. R. L. Mosher and V. R. Knowles, 'Finite element study of tieback wall for Bonneville navigation lock', *Technical Report ITL-90-4*, USAE Waterways Experiment Station, Vicksburg, MS, 1990.
7. D. A. Leavell, J. F. Peters, E. V. Edris and T. L. Holmes, 'Development of finite-element-based design procedure for sheet-pile walls', *Technical Report GL-89-14*, USAE Waterways Experiment Station, Vicksburg, MS, 1989.
8. R. L. Mosher, 'Three-dimensional finite element analysis of sheet-pile cellular cofferdams', *Technical Report ITL-92-1*, USAE Waterways Experiment Station, Vicksburg, MS, 1992.
9. J. M. Duncan and C. Y. Chang, 'Nonlinear analysis of stress and strain in soils', *J. Soil Mech. Found. Div.*, **96**(SM5), 1629–1653 (1970).
10. J. M. Duncan, P. Byrne, K. S. Wong and P. Mabry, 'Strength, stress-strain and bulk modulus parameters for finite element analyses of stresses and movements in soil masses', *Report No. UCB/GT/78-02*, University of California, Berkeley, CA, 1978.
11. A. W. Skempton, 'Standard penetration test procedures and the effects in stands of overburden pressure, relative density, particle size,ageing and overconsolidation', *Geotechnique*, **36**(3), 425–447 (1986)
12. R. M. Ebeling and R. L. Mosher, 'Red river U-frame lock No. 1 backfill-structure-foundation interaction', ASCE, *J. Geotech. Engng.*, **122**(3), 216–225 (1996).
13. M. Peterson, F. Kulhawy, L. Nucci and B. Wasil, 'Stress-deformation behavior of soil-concrete interfaces', Contract Report B-49 to Niagara Mohawk Power Corporation, Syracuse, NY, Dept. of Civil Engrg., Syracuse Univ., Syracuse, NY, 1976.
14. R. D. Holtz and W. D. Kovacs, *An Introduction to Geotechnical Engineering*, Prentice-Hall, Englewood Cliffs, NJ, 1981, 733 p.
15. L. Casagrande, 'Effect of preconsolidation on settlement', *J. Soil Mech. Found. Div.*, **90**(SM5), 349–362 (1964).
16. R. M. Ebeling, J. F. Peters and R. L. Mosher, 'Finite element analysis of slopes with layer reinforement', *Proc. Conf. on Embankment Dams and Slopes*, Vol. 2, *American Society of Civil Engineers Geotechnical Special Publication No. 31*, 1992, pp. 1427–1443.
17. W. P. Doherty, E. L. Wilson and R. L. Taylor, 'Stress analysis of axisymmetric solids utilizing higher-order quadrilateral finite element', *Report No. SESM 69-3*, Structural Engineering Laboratory, University of California, Berkeley, CA, 1969.
18. J. Fowler, R. E. Leach, J. F. Peters and R. C. Hortz, 'Mohicanville reinforced dike no. 2-design memorandum', *Miscellaneous Paper GL-86-26*, USAE Waterways Experiment Station, Vicksburg, MS, 1983.
19. J. T. H. Wu, *Proc. Predictions Symp. on Geosynthetic Reinforced Retaining Walls*, Denver, CO, A.A. Balkema, 1991.
20. R. M. Ebeling, J. F. Peters and R. E. Wahl, 'Prediction of reinforced sand wall performance', *Proc. Predictions Symp. on Geosynthetic Reinforced Retaining Wall*, Denver, CO, A.A. Balkema, 1991, pp. 243–253.
21. R. M. Ebeling, J. F. Peters and R. E. Wahl, 'Lessons learned from deformation analysis of wall experiment', *Proc. Predictions Symp. on Geosynthetic Reinforced Retaining Walls*, Denver, CO, A. A. Balkema, 1991, pp. 255–258.

22. R. E. Goodman, T. L. Taylor and T. L. Breeke, 'A model for the mechanics of joint rock', *J. Soil Mech. Found. Div.*, **94**(SM3), 637–659 (1968).
23. C. S. Desai, L. D. Johnson and C. M. Hargett, 'Finite element analysis of pile-supported locks', *J. Geotech. Engng. Div.* ASCE, **100** (GT9), 1009–1029 (1974).
24. C. S. Desai, M. M. Zaman, J. G. Lightners and H. J. Siriwardane, 'Thin-layer element for interfaces and joint'. *Int. J. Numer. Anal. Methods Geomech.*, **8** (1), 19–43 (1984).

